THE ASTROPHYSICAL JOURNAL, Vol. 157, July 1969

THE SPECTRA OF RADIO SOURCES IN THE REVISED 3C CATALOGUE

K. I. KELLERMANN AND I. I. K. PAULINY-TOTH
National Radio Astronomy Observatory,* Green Bank, West Virginia

AND

P. J. S. WILLIAMS†
Cavendish Laboratory, Cambridge, England
Received October 14, 1968; revised December 16, 1968

ABSTRACT

Accurate values of the flux density are given for nearly all sources in the *Revised Third Cambridge Catalogue* at frequencies of 38, 178, 750, 1400, 2695, and 5000 MHz. These have been used to determine the spectrum of each source over this frequency range. It is concluded that the form of the spectra in many sources is determined not only by the energy distribution of relativistic electrons but also, as a result of self-absorption, by their spatial distribution. Sources identified with quasi-stellar objects have a wider dispersion of spectral indices than those identified with radio galaxies, particularly at the higher frequencies. Among the radio galaxies, the intrinsically strongest sources appear to have the steepest spectra. Unidentified sources have steep spectra similar to those of the stronger radio galaxies, and they are probably distant galaxies.

I. INTRODUCTION

Early studies of the spectra of radio sources were limited by uncertainties in the measurement of flux density, by uncertainties in the calibration of flux-density scales at the different frequencies, and by the limited range of frequencies covered. About 5 years ago observations with large instruments at Cambridge, Caltech, and Jodrell Bank improved the accuracy of flux-density measurements and so made it possible to obtain reasonably accurate spectra for 160 sources over a wide range of frequencies between 38 and 3200 MHz (Conway, Kellermann, and Long 1963, hereinafter referred to as CKL). A uniform flux-density scale was established by CKL at all frequencies by relating the observations to a small number of calibration sources. This scale was then made absolute by comparing these calibration sources with the primary standard source, Cas A, for which absolute flux-density measurements were available over a range of frequencies.

The most important results of the CKL study were the following:

a) For the majority of sources, the flux density S_ν at frequency ν was given by the simple power law, $S_\nu \propto \nu^\alpha$, where α is the spectral index.[1]

b) The extragalactic sources included had a narrow range of spectral indices with a median value of -0.71 and a dispersion of 0.15. For identified extragalactic sources where the redshifts and, therefore, the distances were known, the intrinsically stronger sources were found on the average to have a slightly steeper spectrum. The galactic sources included showed a considerably larger dispersion of spectral indices.

c) The spectra of a number of sources deviated considerably from a simple power law and became significantly steeper as the frequency increased. In a few cases the curvature was so marked that the flux density was found to show a maximum within

* Operated by Associated Universities, Inc., under contract with the National Science Foundation.

† Present address: Adran Ffiseg, Coleg Prifysogol Cymru, Aberystwyth, Wales.

[1] CKL and some other authors define the spectral index α by the power law, $S_\nu \propto \nu^{-\alpha}$.

the range of frequencies observed. Sources with extreme curvature of the spectrum were invariably found to have a small angular size and a high brightness temperature.

The CKL study, however, suffered from several limitations. First, the data were incomplete and subject to strong selection effects. The sources were selected from a low-frequency survey, but only those sources which were strong enough to be observed at the higher frequencies were included. This procedure discriminated against sources with steep spectra because the flux densities of such sources fell below some ill-defined limit at high frequencies. Second, the low primary resolution at several of the frequencies used gave rise to considerable errors in some cases because of confusion by unresolved weaker sources in the antenna beam. Moreover, many of the observations were made with interferometers of moderate spacing, and errors were introduced in some cases by the uncertain corrections for resolution which had to be applied to the observed fringe amplitudes.

A more systematic study of source spectra was based on the observations made with the 210-foot telescope at Parkes, Australia (Bolton, Gardner, and Mackey 1964; Price and Milne 1965; Day *et al.* 1966; Shimmins *et al.* 1966). This covers some 2000 sources south of declination +20° at frequencies of 408, 1410, and 2650 MHz, and the analysis is complete above a limiting flux density of 4 f.u.[2] at the survey frequency of 408 MHz. The number of sources studied at Parkes is much greater than in CKL, but the range of frequencies covered is limited and it is difficult to draw definite conclusions about spectral curvature from measurements at only three frequencies.

Finally, a study has been carried out at Cambridge of the spectra of about 1000 sources from the 4C catalogue in the declination range 0° to +44°, using flux densities measured at frequencies between 38 and 1410 MHz (Long *et al.* 1966; Williams and Stewart 1967; Williams *et al.* 1968) Over the whole range of declinations the analysis is complete above a limiting flux density of 5.0 f.u. at a survey frequency of 178 MHz, while over selected areas of sky the analysis is complete above 15 f.u. at 38 MHz, 2.0 f.u. at 178 MHz, 4.0 f.u. at 408 MHz, and 2.5 f.u. at 610 MHz. The main purpose of this work was to study the statistics of source spectra, the sources being selected at the different frequencies to as low a limiting flux density as possible. In this study less emphasis was given to the detailed analysis of individual spectra.

The present paper attempts to improve the data on the spectra of the stronger radio sources in several respects. Flux densities have now been measured at Cambridge or at the NRAO at 38, 178, 750, 1400, 2695, and 5000 MHz for nearly all sources in the revised 3C catalogue (apart from a few extended sources near the galactic plane), and the data are therefore well suited both for statistical investigation and for the detailed study of individual spectra. At each frequency the flux densities given here are thought to be more reliable than any previously published values. This is due in part to the use of low-noise amplifiers at high frequencies, so that for most of the sources the radiometer noise is not a limiting factor.

One of the greatest difficulties in the determination of radio-source spectra is due to the uncertainty in the flux density of extended sources containing two or more spatially separated components. This is especially true if the observations at the different frequencies have been made with different resolutions. In reporting flux densities obtained at different frequencies, observers often differ in determining which components are to be considered part of the "source" in question. Often the choice is arbitrary, but clearly it must be the same at the different frequencies if relative flux densities or spectral indices are to be meaningful. In the present study the various Parkes catalogues, the 4C catalogue, and the NRAO catalogue (Pauliny-Toth, Wade, and Heeschen 1966) have been used in the interpretation of observations made with less resolution at the lower frequencies. This has greatly improved the homogeneity of the data and minimized errors due to the inclusion of different components at different frequencies.

[2] 1 flux unit = 10^{-26} W m^{-2} Hz^{-1}.

In addition to the improved spectral data, more information is now available about optical identifications, redshifts, brightness distributions, and polarization of discrete sources, so that a more meaningful statistical comparison of the radio spectra with other radio and optical properties can be made. In particular, the whole class of quasi-stellar sources was unrecognized at the time of the CKL study.

In the present paper the discussion is limited to sources in the revised 3C catalogue (Bennett 1962) where the data are nearly complete for the sources at high galactic latitudes; additional papers are in preparation dealing with other sources from the 3C and Parkes catalogues and with the extension of the spectra to shorter wavelengths (Kellermann and Pauliny-Toth 1969).

II. THE OBSERVATIONS

A brief description of the equipment and observing procedure used is given below. A summary of the telescope systems and sources of error at each frequency is given in Table 1. Detailed descriptions will be found elsewhere, as indicated below.

TABLE 1

CHARACTERISTICS OF THE ANTENNA SYSTEMS USED AT THE VARIOUS FREQUENCIES

Frequency (MHz)	Observatory	Instrument	Beam Width	RMS Noise and Confusion (flux units)
38	Cambridge	Pencil-beam aperture-synthesis system	45′×45′ sec ζ	5–10*
178	Cambridge	Pencil-beam aperture-synthesis system	23′×18′ sec ζ	0 5
		3C total power system	0°.2×4°.5	2 0
		4C interferometer aperture synthesis system	25′×35′ sec ζ	0 5
750	Green Bank	300-foot telescope	18′.5×18′.5	0 2
1400	Green Bank	300-foot telescope	10′×10′	0 1
2695	Green Bank	140-foot telescope	11′×11′	0 05
5000	Green Bank	140-foot telescope	6′×6′	0 02–0.05

* According to declination.

a) Observations at the Mullard Radio Astronomy Observatory

i) *38 MHz*

The observations at 38 MHz (λ = 7.9 m) were made with the moving-T aperture-synthesis instrument, which synthesizes a pencil beam of 45′ in right ascension and 45′ sec (ζ) (ζ = zenith angle) in declination (Williams, Kenderdine, and Baldwin 1966). The present flux densities are more accurate than those given in CKL since the full synthesis is now available over the whole sky, whereas previous observations were made with a fan beam of 30′ by 45° for part of the sky, and with only a limited synthesis for the remainder.

ii) *178 MHz*

Where possible, flux densities at 178 MHz (λ = 1.7 m) were taken from observations made with the moving-T aperture-synthesis instrument (Crowther and Clarke 1966), which synthesizes a pencil beam of 23′ in right ascension and 18′ sec (ζ) in declination.

Certain areas of sky, however, were not surveyed by this instrument, and in these regions the most reliable alternative observations, chosen by the following criteria, were used instead:

1. Whenever the flux densities quoted in the revised 3C catalogue were determined

from total power observations, these flux densities were preferred because they include no error due to partial resolution of extended sources.

2. Whenever the revised 3C measurements were made with the interferometer, however, measurements made with the 4C aperture-synthesis interferometer were preferred. Where possible, these were taken from the accurate observations made by Clarke (1965) or by Wills and Parker (1966); otherwise, the flux densities were taken from the 4C catalogue (Pilkington and Scott 1965; Gower, Scott, and Wills 1967).

b) Observations at the National Radio Astronomy Observatory

i) *750 and 1400 MHz*

At 750 (λ = 40 cm) and 1400 MHz (λ = 21 cm), the flux densities were based on the list of Pauliny-Toth, Wade, and Heeschen (1966) (hereinafter referred to as the NRAO list). The observations were made with the 300-foot transit telescope at Green Bank and consisted of drifts of the source through the antenna pattern, with the antenna set to a number of declinations close to that of the source. The beam width was 18′.5 at 750 MHz and 10′.0 at 1400 MHz.

Apart from the readjustment of the flux-density scale discussed in the following section, the flux densities originally quoted have been modified in several ways. It was found that the spectral indices quoted in the NRAO list showed a systematic dependence on declination. A comparison of the data at 1400 MHz with those of Fomalont (1968) showed that, while agreement was excellent for sources below a declination of 50°, at higher declinations the NRAO flux densities were systematically high. The effect is apparently due to an asymmetry in the dependence of the gain of the 300-foot telescope on zenith angle, and was not detected in the original measurements because of the lack of suitable calibration sources in the NRAO list at declinations greater than 52°. The original NRAO flux densities at 1400 MHz have been reduced by 2 per cent in the declination range 50°–70° and by 4 per cent in the declination range 70°–90° to correct for this effect. A second correction was applied to the NRAO measurements at 1400 MHz to allow for polarization. At this frequency the antenna feed was oriented to accept radiation with its electric vector oriented in position angle zero. For 156 of the stronger sources, the polarization measurements of Bologna *et al.* (1965, and private communication), made with the 300-foot telescope at 1410 MHz, were used to correct the NRAO flux densities.

At both 750 and 1400 MHz, the errors given are larger than those quoted in the NRAO list, in which only the uncertainty σ_n due to the receiver noise was considered. The quoted errors have been increased to allow for the effects of confusion, σ_c, and for uncertainties in the correction for the gain of the telescope with zenith angle, σ_g, so that the final uncertainty $\sigma = (\sigma_n^2 + \sigma_c^2 + \sigma_g^2)^{1/2}$. At 750 MHz, σ_c = 0.15 f.u.; at 1400 MHz, σ_c = 0.05 f.u., while σ_g = 1.5 per cent of the flux density at both frequencies.

ii) *2695 and 5000 MHz*

At 2695 MHz (λ = 11 cm) (Kellermann, Pauliny-Toth, and Tyler 1968) and at 5000 MHz (λ = 6 cm) (Pauliny-Toth and Kellermann 1968), the observations were made with the 140-foot telescope, which has beam widths of 11′ and 6′, respectively, at these frequencies. For sources known to be small compared with the beam width and for which accurate radio positions were available, the flux densities were determined by pointing the antenna alternately toward and away from the source and integrating the output of the receiver for 30 seconds in each position. For larger sources, or for sources suspected of being confused by other nearby sources, scans were made in right ascension and declination, and an integrated flux density was determined. All values given at these two frequencies are based on the sum of the antenna temperatures measured in two orthogonal positions of the feed horn and are thus independent of any linear or circular polarization in the sources.

Several strong sources of small angular size were tracked over a range of hour angles in order to determine the change in the gain of the telescope and in the atmospheric extinction with zenith angle. Corrections based on these measurements were applied to the observed antenna temperatures to reduce them to zero zenith angle. The maximum corrections were about 2 per cent at 11 cm and 6 per cent at 6 cm.

III. CALIBRATION OF THE FLUX-DENSITY SCALES

Initially, calibrations at the different frequencies were made independently. At 38 MHz the calibration was absolute, as described by Williams, Kenderdine, and Baldwin (1966). At 178 MHz the flux-density scale was based on CKL. The NRAO observations at 750 and 1400 MHz were based on the scale established by Kellermann (1964), which is close to the CKL scale at these frequencies. In order to obtain a uniform calibration for all the observations, a procedure similar to that used by CKL and by Kellermann was adopted.

Absolute measurements of the flux density of Cas A were plotted for the epoch 1964.4, after correcting for a secular decrease in the flux density of 1.1 per cent per year. Only those measurements where the calibration procedure was adequately described in the literature and which had a claimed accuracy of about 5 per cent or less were used. These data are listed in Table 2, and in Figure 1*a* the data are plotted on a log-log scale. The resulting straight spectrum implies that the spectrum of Cas A follows a simple power law with an index $\alpha = -0.765 \pm 0.005$ between 38 MHz and 15.5 GHz. This is in contradiction to the conclusion of Baars, Mezger, and Wendker (1965), who suggested that the spectrum became steeper at high frequencies, but it is in agreement with more recent measurements at 15.3 GHz by Mezger and Schraml (1966).

The spectra of a number of moderately strong sources were then obtained. For these the 38- and the 178-MHz data were plotted, together with the flux densities at higher frequencies obtained from the spectrum of Cas A derived above and the measurements relative to Cas A by Heeschen (1961), Heeschen and Meredith (1961), Baars, Mezger, and Wendker (1965), Dent and Haddock (1966), and Wilson and Penzias (1966). In doing this, account was taken of the decrease of 1.1 per cent per year in the flux density of Cas A. Of these sources 3C 218 (Hya A), 3C 274 (Vir A), 3C 348 (Her A), and 3C 353 were found to have simple-power-law spectra up to at least 8 GHz (see Fig. 1), and these were therefore chosen as secondary calibration sources. Three of the sources previously used by CKL and by Kellermann for the secondary calibration (viz., 3C 123, 3C 380, and 3C 409) now show significant curvature in their spectra and were rejected as calibration sources.

The best-fitting straight-line spectra for the calibration sources were obtained and were compared at each frequency with the individual data which were then adjusted to obtain the best over-all agreement. At 750 MHz the flux densities quoted in the NRAO list were reduced by 4.5 per cent; at 1400 MHz, by 2 per cent. The standard error in these corrections was $\pm$ 1 per cent. At 2695 and 5000 MHz this procedure was used to calibrate the flux-density scales. (On this scale, the flux densities of Dent and Haddock [1966] at 8 GHz, which were based on a low value for Cas A, should be increased by 11 per cent.) Allowing for the uncertainty in the absolute measurements of Cas A and in the relative measurements, it is felt that the systematic errors in the flux-density scales at 750 MHz and higher frequencies are less that $\pm$ 5 per cent in each case.

At lower frequencies the accuracy in the absolute measurements of Cas A and in the ratio of Cas A to the secondary calibrators is considerably poorer. The calibration at 38 and 178 MHz, obtained in the manner described above, does not differ significantly from the CKL scale. Recent measurements at 81.5 MHz (Collins, unpublished) and 408 MHz (Wyllie 1969) indicate that the CKL flux scale may be 5 or 10 per cent low at 38 and 178 MHz. This would be in closer agreement with the scales established by Kellermann (1964), which were higher than CKL by 8 per cent at 38 and 178 MHz. In view

TABLE 2

FLUX DENSITY OF CASSIOPEIA A*

Frequency (MHz)	Flux Density (10^{-26} W m^{-2} Hz^{-1})	Reference
38 .	37,200±3.7%	Parker (1968)
81.5	21,680±2 9%	Parker (1968)
152	13,130±2.9%	Parker (1968)
320	7,680±5.0%	MacRae and Seaquist (1963)
562 . . .	4,855±3.0%	Lastochkin *et al.* (1963)
708 .	4,085±2.5%	
860 . .	3,295±2.5%	
1190	2,985±4 0%	
1440	2,335±2 1%	Findlay, Hvatum, and Waltman (1965)
2924	1,495±3 3%	Khrulev (1963)
3060	1,415±4 0%	Stankevich (1963)
3150	1,260±4 0%	Medd and Ramana (1965)
4080	1,080±3 0%	Penzias and Wilson (1965)
8250 .	620±4 8%	Allen and Barrett (1967)
15500	380±5.2%	Allen and Barrett (1967)

* Corrected to epoch 1964.4.

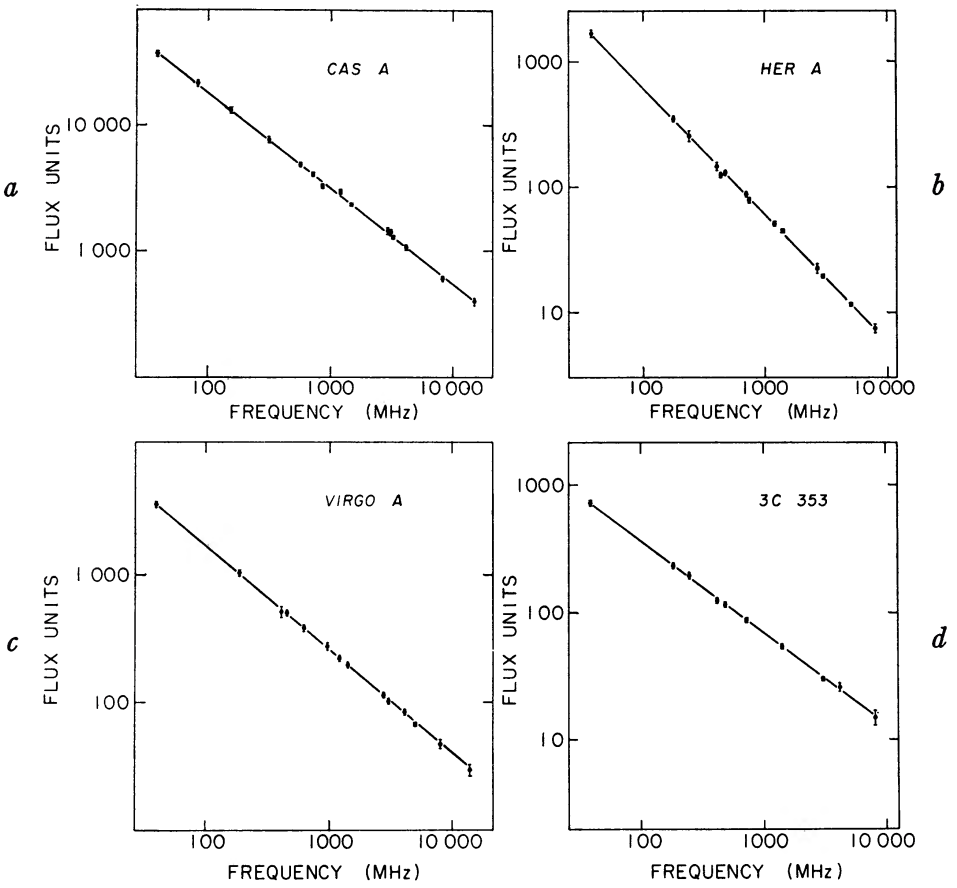

FIG. 1.—Spectra of calibration sources: (*a*) Cas A (3C 461) based on absolute flux densities corrected to the epoch 1964.4; (*b*) Her A (3C 348) based on ratios to Cas A; (*c*) Vir A (3C 274) based on ratios to Cas A; (*d*) 3C 353 based on ratios to Cas A.

of the still large uncertainties in the low-frequency calibration and since the CKL scale has been so widely used, we have retained this scale below 750 MHz. The uncertainty is estimated to be ± 10 per cent at 178 MHz and ±15 per cent at 38 MHz.

IV. THE FLUX DENSITIES

The flux densities used in deriving the spectra are presented in Table 3. Column (1) gives the source number in the revised 3C catalogue, and columns (2)–(7) give the measured flux densities at each frequency.[3] Estimates of the standard errors in the quoted flux densities are indicated by the following symbols: (*a*) $\sigma < 5$ per cent; (*b*) 5 per cent $< \sigma <$ 15 per cent; (*c*) 15 per cent $< \sigma <$ 25 per cent; (*d*) 25 per cent $< \sigma <$ 35 per cent; (*e*) 35 per cent $< \sigma$. These errors include the random errors in the relative flux densities due to receiver noise, confusion, resolution, and gain uncertainties. They do not include the uncertainty in the calibration of the flux-density scales at each frequency as described above. Flux densities which have been observed to vary with time are all noted with asterisks and correspond to the epoch 1967.0.

The flux densities at 178 MHz have a superscript which indicates the source of the measurements. The symbol 3 indicates that the flux density was taken from the 3C catalogue, the symbol 4 indicates that the flux density was taken from the 4C catalogue, and the symbol 4′ indicates that the flux density was based on the accurate observations made by Clarke (1965) or by Wills and Parker (1966) with the 4C aperture-synthesis interferometer. No symbol is used if the flux density was measured with the pencil-beam synthesis instrument.

In the case of complex sources containing two or more widely separated components, or where there are nearby sources, a footnote describes specifically which components were and which were not included in the quoted flux densities. The different components are described by their 4C, NRAO, and Parkes catalogue numbers.

V. THE SPECTRA

In previous surveys of spectra, where the flux densities were quoted with large errors and where the frequency ranges covered were limited, it was usually possible to represent the spectra of sources by a simple power law: $S_\nu \propto \nu^\alpha$. In the present study the errors in flux density are smaller and the range of frequencies covered is considerably increased, so that it is generally not possible to represent each spectrum adequately by a single parameter. Several two-parameter solutions were therefore considered. The simple parabolic form,

$$\log (S_\nu) = \alpha \log (\nu) + \beta \log^2 (\nu) + \text{const.},$$

used by Howard *et al.* (1965) was rejected, since when $\log (S_\nu)$ is plotted against $\log (\nu)$, it is obvious that in most cases the curvature is neither continuous nor parabolic. At the higher frequencies the spectrum can usually be represented by a constant spectral index; at the lower frequencies, either the spectra can be represented by a constant but different index generally smaller than at high frequencies, or they show pronounced curvature. In a few cases the curvature is so great that the flux density reaches a maximum at some frequency and rapidly decreases below this frequency.

There is clearly no simple form that can be used to represent all radio spectra. We therefore chose to fit the spectrum of each source over two ranges of frequency, using two power-law spectra with different indices; the ranges chosen were 38–750 and 750–5000 MHz. Within each range a straight line was fitted to a logarithmic plot of the data by a least-squares procedure, each point being weighted according to the total uncer-

[3] At 2695 MHz, some of the flux densities given by Kellermann, Pauliny-Toth, and Tyler (1968) have been revised here, on the basis of more recent information.

Table 3

The Flux Densities

Source	S_{38}	S_{178}	S_{750}	S_{1400}	S_{2695}	S_{5000}	Notes
3C 2	44 c	14.9[4'] b	5.7 a	3.5 a	2.25 a	1.41 a	
3C 6.1		17.3[3] b	5.4 a	3.4 a	1.85 a	1.04 a	1
3C 9	64 b	17.8 a	3.7 b	1.9 b	0.97 b	0.55 b	
3C 10	445 c	145.0[3] a	60.1 a	41.9 a	28.9 a	21.3 a	
3C 11.1	80 d	12.4[3] c	5.4 a	2.8 a	1.64 a	0.82 a	
3C 13	57 c	12.0 a	3.3 b	1.8 b	0.91 b	0.40 b	
3C 14	36 c	10.4[4] b	3.4 b	1.9 b	1.01 a	0.61 b	
3C 14.1		16.1[4] b	4.9 a	2.6 a	1.24 a	0.67 a	2
3C 15	42 c	15.8[4] a	6.3 a	4.3 a	2.40 a	1.61 a	
3C 16	31 c	11.2 a	3.0 b	1.8 b	0.94 b	0.51 b	
3C 17	70 b	20.0[4] b	9.5 a	6.2 a	3.83 a	2.72 b	
3C 18	45 b	19.0 a	6.6 a	4.3 a	2.65 a	1.73 a	
3C 19	35 d	12.1[4] b	5.1 a	3.1 b	1.88 a	1.26 b	
3C 20	112 d	42.9 a	17.3 a	11.8 a	6.43 a	4.18 a	
3C 22	40 d	12.1 a	4.1 a	2.3 b	1.28 a	0.76 a	
3C 27	59 d	26.5 a	10.7 a	7.3 a	4.26 a	2.48 a	
3C 28	76 b	16.3[4] b	3.7 b	1.8 b	0.67 b	0.45 b	
3C 29	89 c	15.1[4] b	7.4 a	4.8 a	3.37 a	2.16 a	3
3C 31	54 b	16.8 a	7.7 a	4.9 a	3.49 b	2.10 a	
3C 33	137 a	54.4[3] a	19.1 a	13.3 a	7.92 a	5.04 b	
3C 33.1	41 c	13.0 b	5.1 b	3.0 b	1.73 a	0.86 a	
3C 33.2		5.5 b	1.5 b	0.9 b	0.52 b	0.30 b	
3C 34	63 b	11.9[3] b	2.7 b	1.6 b	0.80 b	0.43 b	
3C 35	55 b	10.5 b	3.6 b	2.1 b	1.33 a	0.59 b	
3C 36	37 c	8.2 b	2.4 b	1.2 b	0.63 b	0.36 b	
3C 40	102 b	26.0[3] b	10.0 a	4.9 a	3.21 a	1.88 a	4
3C 41	37 c	10.6[4] b	5.3 a	3.5 a	2.23 a	1.46 a	
3C 42	35 c	12.0[4'] a	4.4 a	2.6 a	1.59 a	0.84 b	
3C 43	39 c	11.6 b	4.1 a	2.7 a	1.68 a	1.09 a	
3C 44	42 b	7.9 b	2.4 b	1.3 b	0.67 b		
3C 46	33 c	10.2 a	2.1 b	1.1 b	0.65 b	0.33 c	
3C 47	125 b	26.4[4] b	6.7 a	3.6 a	2.06 a	1.10 a	
3C 48	61 b	55.0[4'] a	24.4 a	15.3 a	8.97 a	5.37 a	
3C 49	≤6	10.3 a	4.2 a	2.7 a	1.51 a	0.94 b	
3C 52	27 c	13.5 a	5.5 a	3.8 a	2.30 a	1.48 a	
3C 54	35 c	8.8 b	2.7 b	1.8 b	0.96 b	0.60 b	
3C 55	76 b	22.7[3] b	5.0 a	2.6 a	1.47 a	0.88 b	
3C 58		28.5 a	33.3 a	32.6 a	30.6 a	27.2 a	5
3C 61.1	87 b	31.2[3] b	10.7 a	5.8 a	3.15 a	1.91 a	
3C 63	78 b	19.2[4'] b	6.2 a	3.2 a	1.83 a	1.09 b	

Table 3 (Continued)

Source	S_{38}	S_{178}	S_{750}	S_{1400}	S_{2695}	S_{5000}	Notes
3C 65	55 b	15.2[4] b	5.4 a	3.1 b	1.44 a	0.77 b	
3C 66	125 a	35.7[3] a	14.7 a	9.8 a	6.31 a	3.75 a	
3C 67		10.0[4'] a	4.5 a	2.9 b	1.68 a	0.91 b	
3C 68.1	47 b	12.8[4'] b	4.2 a	2.5 b	1.38 a	0.83 a	
3C 68.2	63 b	13.0[3] b	2.3 b	1.0 b	0.41 b	0.18 c	
3C 69	73 b	20.9 a	5.7 b	3.4 a	1.70 a	0.87 b	
3C 71	33 c	16.1[4] b	7.3 a	4.9 a	2.99 a	1.90 a	
3C 75	92 b	25.8 a	9.3 a	6.2 a	3.61 a	2.36 b	
3C 76.1	25 d	12.2 a	4.2 a	2.9 a	1.94 a	1.31 a	
3C 78	52 b	17.8 a	9.6 a	7.1 a	5.05 a	3.40 a	
3C 79	75 b	30.5 a	8.5 a	4.4 b	2.45 a	1.31 a	
3C 83.1	110 a	30.2[3] b	12.0 a	8.2 a	4.87 a	3.53 b	
3C 84	360 a	62.6[3] a	20.8*a	12.7*a	9.9 *a	18.0 *a	
3C 86	80 a	29.0 a	11.5 a	8.1 a	5.06 a	3.85 b	6
3C 88	48 b	15.3 a	7.2 a	4.7 a	2.98 a	1.96 b	
3C 89	102 b	20.2[4] b	5.1 a	2.7 a	1.42 a	0.81 b	
3C 91	34 b	14.1 a	5.0 a	3.3 a	1.97 a	1.16 a	
3C 93	36 c	14.4 a	4.4 a	2.8 a	1.58 a	0.89 a	
3C 93.1	21 d	9.9 b	3.6 b	2.3 a	1.28 a	0.75 b	
3C 98	147 a	47.2 a	16.0 a	9.9 a	7.01 a	4.97 a	
3C 99	16 f	10.8[3] b	2.4 b	1.6 b	0.91 b	0.69 a	
3C 103	88 b	26.6[4] b	8.5 a	5.2 b	2.56 b	1.41 a	
3C 105	54 b	17.8 a	7.7 a	5.1 b	3.36 a	2.16 a	
3C 107	27 d	10.8[4'] b	2.5 b	1.5 b	0.74 b	0.36 b	
3C 109	59 b	21.6 a	6.6 a	4.0 a	2.43 a	1.64 b	
3C 111	218 a	64.6 a	22.7 a	14.8 a	10.46 a	7.87 a	
3C 114	28 d	6.5 b	1.8 b	1.0 b	0.49 b	0.33 b	
3C 119	18 d	15.7 a	11.5 a	8.3 a	5.36 a	3.42 a	
3C 123	577 a	189.0[3] a	72.3 a	45.9 a	27.2 a	16.32 a	
3C 124	18 e	10.3[3] c	1.9 b	1.2 b	0.55 b	0.34 b	
3C 125	52 b	14.1[4] a	3.6 b	2.2 a	0.98 b	0.55 a	
3C 129	175 b	46.9 a	12.5 a	8.0 a	4.11 b	2.16 a	7
3C 130	50 b	15.5 b	4.3 a	2.6 a	1.58 a	0.89 b	
3C 131	48 b	14.6[3] b	4.7 a	2.9 a	1.48 d	0.86 a	
3C 132	44 b	13.7 a	5.4 a	3.2 a	1.94 a	1.05 a	
3C 133	58 b	22.3[4'] a	8.5 a	5.7 a	3.38 a	2.16 a	
3C 134	313 a	74.4 a	18.0 a	9.1 a	4.25 a	1.95 a	
3C 135	48 b	17.3[3] b	4.6 a	3.3 b	1.72 b	1.08 b	8
3C 136.1	66 b	14.0[3] b	5.2 b	2.9 b	2.08 a	1.41 a	
3C 137	29 c	12.5 a	3.3 b	2.3 a	1.06 a	0.57 b	

Table 3 (Continued)

Source	S_{38}	S_{178}	S_{750}	S_{1400}	S_{2695}	S_{5000}	Notes
3C 138	13 e	22.2 a	12.0 a	9.2 a	5.99 a	4.16 c	
3C 139.1	≲5	21.6[3] b	37.7 b	39.1 b			9
3C 139.2	58 b	11.9[3] c	3.0 b	1.5 b	1.03 a	0.65 b	
3C 141	52 b	14.9[4'] a	4.2 a	2.0 a	1.11 a	0.55 c	
3C 142.1	86 b	19.4 a	5.6 a	3.6 b	1.72 a	1.02 a	
3C 144	2430 a	1534.0[3] a		930. a		680. a	10
3C 147	18 d	60.5 a	32.6 a	22.2 a	12.98 a	8.18 a	
3C 147.1	≲6	15.7[3] b	53.3 a	63.4 a	60.0 a	51.6 b	11
3C 152	31 c	12.4[4] b	3.5 b	1.5 b	0.84 b	0.25 b	
3C 153	40 b	15.3 a	6.2 a	4.2 a	2.30 a	1.35 a	
3C 153.1	17 e	20.5[3] b	29.9 a	28.5 a			12
3C 154	78 b	23.1[4] b	7.6 a	5.2 a	3.07 a	2.02 a	
3C 157	460 a	227.0[3] c	190. b	170. b	130. c		13
3C 158	63 b	18.1 a	3.8 a	2.2 a	1.11 a	0.63 b	
3C 165	46 b	13.5[4] b	4.9 a	2.7 b	1.33 a	0.77 a	
3C 166	73 b	14.7[4] b	4.0 a	2.6 a	1.69 a	1.12 a	
3C 169.1	29 c	7.3 b	2.0 b	1.2 b	0.52 b	0.40 b	
3C 171	49 b	19.5 a	5.8 a	3.7 a	2.00 a	1.22 a	
3C 172	41 b	15.1 b	4.6 a	2.7 a	1.51 a	0.85 a	
3C 173	17 d	8.7 b	3.1 b	1.8 b	0.86 b	0.52 b	
3C 173.1	48 b	15.4 a	4.5 a	2.6 a	1.44 a	0.77 b	
3C 175	81 b	17.6 a	4.5 a	2.5 a	1.23 a	0.66 b	
3C 175.1	19 d	11.4 a	3.2 b	2.1 a	1.10 a	0.56 b	
3C 177	25 c	8.7 b	2.1 b	1.4 b	0.76 b	0.38 b	14
3C 180	49 c	15.1[3] b	4.5 a	2.6 a	1.59 a	0.94 a	
3C 181	32 c	14.5 a	3.6 b	2.3 a	1.24 a	0.66 b	
3C 184	30 c	13.2 a	4.0 a	2.4 a	1.17 a	0.60 b	
3C 184.1	37 b	13.0[3] b	5.1 a	3.2 a	1.95 a	1.24 b	
3C 186	49 b	14.1 a	2.6 b	1.4 b	0.58 b	0.38 b	
3C 187	53 b	8.1 b	2.5 b	1.6 b	0.75 b	0.39 b	
3C 190	34 c	15.0 a	4.1 a	2.6 a	1.38 a	0.82 b	
3C 191	48 b	13.0[4'] a	3.3 b	1.7 b	0.95 b	0.46 b	
3C 192	79 b	21.0[3] b	7.6 a	4.7 a	3.16 a	2.05 a	
3C 194	28 c	9.9[4] b	3.2 b	2.1 a	1.07 a	0.61 b	
3C 196	166 a	68.2 a	22.8 a	13.9 a	7.66 a	4.36 a	
3C 196.1	91 b	18.6[4] b	3.5 b	1.8 b	0.76 b	0.47 b	
3C 197.1	24 c	8.1 b	3.0 b	1.9 b	1.16 a	0.86 b	
3C 198	45 b	9.7 b	3.6 b	2.1 a	0.98 b	0.46 b	
3C 200	41 b	14.0[3] b	3.5 b	2.0 a	1.10 a	0.66 a	
3C 204	45 b	10.5 a	2.3 b	1.3 b	0.50 b	0.34 b	

Table 3 (Continued)

Source	S_{38}	S_{178}	S_{750}	S_{1400}	S_{2695}	S_{5000}	Notes
3C 205	46 b	12.6 b	3.7 b	2.4 a	1.11 a	0.67 b	
3C 207	37 c	13.6 a	3.9 a	2.6 a	1.78 a	1.44 a	
3C 208	58 b	18.5[4] a	4.4 a	2.2 a	1.25 b	0.54 b	
3C 208.1	16 e	8.1[4] b	3.2 b	2.1 a	1.22 a	0.71 b	
3C 210	34 c	9.5[4] b	3.1 b	1.7 b	0.93 b	0.49 c	
3C 212	22 d	15.1 a	4.2 a	2.6 a	1.41 a	0.89 a	
3C 213.1	17 f	6.6[4] b	3.0 b	1.9 b	1.01 a	0.84 a	
3C 215	36 c	11.4 a	2.6 b	1.6 b	0.70 b	0.41 b	
3C 216	51 b	20.2[4] b	6.3 a	3.7 a	2.39 a	1.81 a	
3C 217	39 b	11.3 a	3.9 a	2.2 a	1.00 a	0.48 b	
3C 219	118 a	41.2 a	13.4 a	7.7 a	4.35 a	2.29 a	
3C 220.1	46 b	15.8[4] b	4.3 a	2.2 a	1.07 a	0.54 b	
3C 220.2	19 d	7.2 b	3.0 b	1.8 b	0.99 b	0.59 b	
3C 220.3	42 b	15.7[3] b	5.6 b	2.8 a	1.33 a	0.64 b	
3C 222	24 d	11.3 a	2.1 b	1.0 b	0.28 c	0.13 c	
3C 223	44 b	14.7 a	5.3 a	3.1 a	2.06 a	1.29 b	
3C 223.1	17 d	6.0 b	2.7 b	1.9 b	1.23 a	0.87 b	
3C 225	55 b	28.9 a	7.6 a	4.3 a	2.22 a	1.26 b	15
3C 226	48 b	15.0 a	4.4 a	2.2 a	1.22 a	0.64 b	
3C 227	124 a	30.4 a	11.6 a	6.8 a	4.16 a	2.60 a	
3C 228	45 b	21.8 a	5.4 a	3.5 a	1.98 a	1.14 b	
3C 230	76 b	21.1 a	6.5 a	3.8 b	1.94 a		16
3C 231	23 c	14.6 a	10.2 a	8.4 a	5.59 a	3.94 a	17
3C 234	114 b	31.4 b	9.5 a	5.2 a	2.92 a	1.54 a	
3C 236		11.3 a		3.2 b	2.01 a	1.34 b	18
3C 237	30 c	20.9 a	9.8 a	6.3 a	3.66 a	2.01 a	
3C 238	44 b	16.6 a	5.1 a	2.6 a	1.35 a	0.58 b	
3C 239	50 b	13.2 a	2.9 b	1.4 b	0.65 b	0.33 b	
3C 241		11.6 a	3.0 b	1.7 b	0.73 b	0.34 c	
3C 244.1	73 b	20.3 a	6.5 a	3.8 a	1.95 a	1.12 a	
3C 245	40 b	14.4 a	4.9 a	3.2 a	2.09 a	1.39 a	
3C 247	22 c	16.8[3] b	4.6 a	2.8 a	1.63 a	0.95 b	
3C 249	37 c	16.9 a	4.7 a	2.6 a	1.29 a	0.61 c	
3C 249.1	39 c	12.5[3] b	3.5 b	2.3 a	1.40 a	0.78 a	
3C 250	48 b	11.9[3] b	2.5 b	1.2 b	0.49 b	0.29 b	
3C 252	67 b	11.0 a	2.6 b	1.2 b	0.58 b	0.32 b	
3C 254	61 b	19.9[4] b	5.2 a	3.1 a	1.45 a	0.79 b	
3C 255	24 d	12.5 b	3.6 b	1.7 b	0.55 b	0.19 c	
3C 256	35 c	9.3[4] b	2.6 b	1.4 b	0.62 b	0.38 b	
3C 257	36 c	9.7[3] c	2.9 b	1.7 b	0.86 b	0.52 b	

Table 3 (Continued)

Source	S_{38}	S_{178}	S_{750}	S_{1400}	S_{2695}	S_{5000}	Notes
3C 258		9.7[3] c	1.5 b	1.1 b	0.59 b	0.40 b	
3C 263	46 b	15.2 a	4.9 a	2.9 a	1.73 a	1.04 a	
3C 263.1	45 b	18.2 a	5.4 a	2.9 a	1.49 a	0.78 a	
3C 264	96 b	26.0 a	9.2 a	5.8 b	3.24 a	2.00 a	
3C 265	77 b	19.5[3] b	5.1 a	2.8 a	1.39 a	0.63 b	
3C 266	28 c	11.1 a	2.7 b	1.5 b	0.58 b	0.32 b	
3C 267	41 c	14.6[3] b	4.0 a	2.2 a	1.29 a	0.59 b	
3C 268.1	51 b	21.4 a	9.6 a	6.6 a	4.00 a	2.62 a	
3C 268.2	34 c	9.7[3] c	2.3 b	1.5 b	0.73 b	0.38 b	
3C 268.3		10.7 a	5.4 a	3.5 a	1.98 a	1.09 a	
3C 268.4	31 c	10.3[3] a	3.4 b	2.3 a	1.06 a	0.60 b	
3C 270	122 a	51.8 a	24.9 a	18.1 a	12.65 a	8.32 a	
3C 270.1	28 c	13.6 a	4.8 a	2.6 a	1.49 a	0.87 a	
3C 272	16 e	10.3 c	2.4 b	1.8 b	0.70 b	0.36 b	
3C 272.1	46 c	19.5[3] b	8.5 a	5.9 a	3.91 a	2.86 a	
3C 273	≳140	62.8 a	45.3*a	45.0*a	41.8 *a	44.9 *a	19
3C 274	3570 a	1050.[3] a	352. a	214. a	118.[3] a	72.1 a	20
3C 274.1	58 b	16.5 a	4.9 a	2.9 a	1.44 a	0.76 a	
3C 275	21 e	14.5[4]' b	5.5 a	3.3 a	1.85 a	0.95 b	
3C 275.1	40 c	18.3 a	4.8 a	2.8 a	1.56 a	0.91 b	
3C 277	31 c	7.5 b	2.1 b	1.3 b	0.60 b	0.31 c	
3C 277.1	13 e	8.5 b	3.4 b	2.5 a	1.53 a	1.05 a	
3C 277.2	48 c	12.0 a	2.9 b	2.0 a	0.91 b	0.58 b	
3C 277.3	33 c	12.4[3] b	4.1 a	3.0 a	1.93 a	1.24 a	
3C 280	62 b	23.7 a	7.7 a	4.9 a	2.83 a	1.53 a	
3C 280.1	27 c	11.9[3] b	2.5 b	1.5 b	0.62 a	0.36 b	
3C 284	46 b	11.4[3] b	3.0 b	1.9 b	1.07 a	0.69 b	
3C 285	36 b	11.4[3] b	3.0 b	2.2 a	1.23 a	0.76 b	
3C 286	32 c	24.0[4] b	18.4 a	14.4 a	10.26 a	7.48 a	21
3C 287	26 c	16.0[4] a	9.3 a	6.9 a	4.60 a	3.26 a	22
3C 287.1	37 c	8.2 b	3.9 a	3.0 a	1.92 a	1.43 b	
3C 288	47 b	18.9 a	5.8 a	3.4 a	1.76 a	0.99 b	
3C 288.1	23 c	9.0 b	2.7 b	1.5 b	0.81 b	0.40 b	
3C 289	29 b	12.0 a	3.9 a	2.4 a	1.17 a	0.60 b	
3C 293	42 b	12.7 b	6.9 a	4.5 a	2.89 a	1.87 a	23
3C 293.1	42 c	9.2 b	2.2 b	1.1 b	0.49 b		
3C 294	63 b	10.3 a	2.3 b	1.3 b	0.54 b	0.28 c	
3C 295	94 a	83.5 a	35.3 a	22.7 a	11.83 a	6.53 a	
3C 296	26 d	13.0 a	5.2 a	4.3 a	2.70 a	1.71 a	
3C 297	50 c	10.3 b	2.5 b	1.5 b	1.00 b	0.64 a	

Table 3 (Continued)

Source	S_{38}	S_{178}	S_{750}	S_{1400}	S_{2695}	S_{5000}	Notes
3C 298	73 b	47.5 a	11.5 a	5.7 a	2.71 a	1.46 a	
3C 299	29 c	11.8[4]' b	4.8 a	2.7 a	1.59 a	0.90 b	
3C 300	67 b	17.9 a	6.1 a	3.6 a	1.92 a	1.10 a	
3C 300.1	41 c	14.1 a	5.3 a	3.3 b	1.83 a	0.94 a	
3C 303	37 b	11.2 a	3.9 a	2.4 a	1.55 a	0.94 b	
3C 303.1	13 e	12.4[3] b	2.8 b	1.9 b	0.61 b	0.46 b	24
3C 305	49 b	15.7 a	4.8 a	3.0 a	1.64 a	0.92 a	
3C 305.1	13 e	12.4[3] b	2.4 b	1.7 b	0.77 b	0.46 b	25
3C 306.1	38 c	13.5[3] b	3.7 b	1.9 b	1.13 a	0.75 b	25
3C 309.1	37 b	22.7 a	11.0 a	7.9 a	5.30 a	3.76 a	
3C 310	218 a	56.0[3] a	15.2 a	7.7 a	3.10 a	1.28 b	
3C 313	81 b	20.6 a	6.3 a	3.5 a	2.07 a	1.39 a	
3C 314.1	43 b	10.6 a	2.8 b	1.6 b	0.70 b	0.33 b	
3C 315	73 b	18.9[3] b	6.6 a	4.0 a	2.36 a	1.27 a	26
3C 317	165 b	49.0 a	11.3 a	5.4 a	2.11 a	0.87 a	
3C 318	22 d	12.3 a	4.2 a	2.6 a	1.33 a	0.75 a	
3C 318.1	119 b	11.3 a	0.7 d	< 0.1	< 0.04	< 0.03	27
3C 319	47 b	15.3 a	4.4 a	2.5 a	1.25 a	0.65 a	
3C 320	26 c	9.1 b	3.1 b	1.7 b	0.91 b	0.50 b	
3C 321	58 b	13.5[3] b	5.9 a	3.4 a	2.03 a	1.22 b	28
3C 322	29 b	10.1 a	3.3 b	2.0 a	0.85 b	0.46 b	
3C 323	31 c	8.4 b	2.5 b	1.3 b	0.65 b	0.33 c	
3C 323.1	24 d	9.7[3] c	3.8 a	2.4 a	1.29 a	0.92 b	
3C 324	49 b	15.8 a	4.5 a	2.6 a	1.26 a	0.61 b	
3C 325	36 b	15.6 a	5.9 a	3.7 a	1.84 a	0.83 b	
3C 326	78 b	12.1 a	6.6 a	3.1 b	2.07 b		29
3C 326.1	41 b	8.2 b	6.8 a	3.0 b	1.35 a	0.86 b	30
3C 327	162 b	35.3 a	14.6 a	8.6 a	5.21 a	2.76 a	31
3C 327.1	86 c	23.6 a	7.4 a	4.1 a	2.10 a	1.10 a	
3C 330	81 b	27.8 a	10.4 a	6.9 a	3.76 a	2.35 a	
3C 332	30 c	9.6 b	4.0 a	2.5 a	1.46 a	0.83 a	
3C 334	71 b	10.9 a	3.3 b	2.2 a	1.32 a	0.57 b	
3C 336	40 b	11.5[4]' b	4.2 a	2.6 a	1.39 a	0.69 b	
3C 337	28 c	11.8 a	5.0 a	3.2 b	1.57 a	0.91 a	
3C 338	220 a	46.9 a	8.8 a	3.5 a	1.24 a	0.49 b	
3C 340	36 c	10.1 a	3.7 b	2.3 a	1.35 a	0.69 a	
3C 341	36 c	10.8 b	3.3 b	2.1 a	1.08 a	0.57 b	
3C 343	≲8	12.4 a	7.6 a	4.9 a	2.68 a	1.49 a	32
3C 343.1	8 f	11.5 a	7.6 a	4.1 a	2.23 a	1.20 a	32
3C 345	24 c	10.8[4]' a	7.6 a	6.6*a	5.3 *a	5.5 *a	33

Table 3 (Continued)

Source	S_{38}	S_{178}	S_{750}	S_{1400}	S_{2695}	S_{5000}	Notes
3C 346	35 c	10.9 a	5.4 a	3.6 a	2.33 a	1.63 b	
3C 348	1690 a	351.0[3] a	83.7 a	44.5 a	22.4 a	11.89 a	
3C 349	50 b	13.3 a	4.8 a	3.2 a	1.88 a	1.14 a	
3C 351	40 b	13.7 a	5.0 a	3.2 a	2.03 a	1.21 a	
3C 352	42 c	11.3 a	3.3 b	2.0 a	0.95 b	0.47 b	
3C 353	713 a	236.0 a	84.5 a	54.9 a	34.8 a	21.5 a	
3C 356	48 b	11.3 a	2.7 b	1.4 b	0.66 b	0.38 b	
3C 357	30 d	9.7[3] c	4.3 b	2.7 b	1.80 a	1.00 a	
3C 368	54 d	13.8 a	2.4 b	1.1 b	0.43 b	0.21 b	
3C 371	15 e	3.7 b	2.4 b	2.6*a	1.92*a	1.74*a	34
3C 379.1	33 c	7.4 b	2.8 b	1.7 b	1.10 a	0.66 b	
3C 380	211 a	59.4 a	22.2 a	14.8*a	10.1 *a	7.5 *a	35
3C 381	35 b	16.6 a	5.4 b	3.8 b	2.30 a	1.29 a	
3C 382	92 c	19.9 a	8.9 b	5.6 b	3.49 a	2.22 a	36
3C 386	72 d	23.9 a	10.5 a	7.0 a	4.32 a	2.58 a	
3C 388	65 b	24.6 a	9.4 a	5.6 a	3.11 a	1.77 a	
3C 390	81 c	21.0 a	7.6 a	4.6 a	2.79 a	1.77 a	
3C 390.3	120 d	47.5[3] a	16.8 a	11.6 a	6.76 a	4.48 a	37
3C 391		17.0 a	28.1 b	20.2 a	13.6 a	10.07 b	
3C 392	766 d	378.0 b	231.4 b	167.8 b			38
3C 394		15.1 a	4.9 a	2.6 a	1.50 a	0.96 b	39
3C 396		23.8[3] b	16.5 b	13.4 a		10.05 a	40
3C 396.1	50 d	32.4[3] b	12.0 c	9.0 c			41
3C 397	40 d	62.0 c	40.2 b	28.4 c	19.6 c	15.2 c	42
3C 398		68.0 a	44.3 c	35.8 b		14.7 b	43
3C 399.1	79 d	13.5[3] b	4.4 a	2.6 a	1.67 a		44
3C 399.2	100 d	42.0 b	23.5 b	16.9 b			
3C 400	≤15	310.0 b	643.4 b	565.1 b			45
3C 400.1		12.4 a	3.7 b	2.3 a	1.40 a	0.93 b	
3C 400.2	57 c	21.0 b	8.5 a	6.7 b			
3C 401		20.9 a	7.8 a	4.7 a	2.76 a	1.37 a	
3C 402		10.1 a	4.5 a	3.0 a	1.80 a	0.92 b	
3C 403	78 d	17.8 a	9.3 a	5.9 a	3.57 a	2.07 a	
3C 403.1	48 d	13.5[3] b	2.7 b	1.8 b	0.96 b	0.45 c	
3C 403.2		54.0[3] b	71.7 b	73.6 b	39.4 c		46
3C 405	22000 b	8700.[3] b	2980. a	1590.	785. a	371. a	47
3C 409	280 d	76.6 a	25.1 a	13.9 a	6.44 a	3.12 a	
3C 410	96 d	34.6 b	15.5 a	10.1 a	6.00 a	3.79 a	
3C 411	59 d	16.5 a	5.3 a	3.2 a	1.69 a	0.87 b	
3C 415.2		8.8 b	2.0 b	1.1 b	0.56 b	0.32 c	

Table 3 (Continued)

Source	S_{38}	S_{178}	S_{750}	S_{1400}	S_{2695}	S_{5000}	Notes
3C 418		13.1 a	7.0 a	5.3*b	4.71*a	3.81*a	48
3C 424	57 c	14.6 a	4.3 b	2.2 a	1.22 a	0.65 a	
3C 427.1	93 d	26.6 a	6.9 a	3.7 a	1.89 a	0.96 b	
3C 428	74 c	16.6 a	6.4 a	2.9 b	1.48 a	0.43 b	49
3C 430	126 d	33.7 a	11.9 a	7.5 a	4.69 a	3.32 a	
3C 431	115 d	24.2 a	6.3 a	3.1 a	1.56 a	0.86 b	
3C 432	47 c	11.0[4'] b	2.8 b	1.5 b	0.76 b	0.31 c	
3C 433	187 d	56.2[3] a	19.9 a	11.5 a	6.49 a	3.74 a	
3C 434	17 f	4.8[4] b	2.0 b	1.2 b	0.75 b	0.39 b	
3C 434.1	58 d	32.0 a	12.0 b	11.4 b			50
3C 435	37 d	11.6 a	3.3 b	2.1 a	1.06 a		
3C 435.1		12.0 b	5.6 b	3.1 b	1.45 a		51
3C 436	87 d	17.8[4'] a	5.4 a	3.2 a	1.82 a	0.99 a	
3C 437	43 c	14.6 a	4.9 a	2.8 a	1.51 a	0.88 b	
3C 437.1	28 c	16.2 b	4.9 b	3.3 b			52
3C 438	138 d	44.7 a	13.1 a	6.8 a	3.22 a	1.54 a	
3C 441	41 c	12.6[4'] b	4.0 a	2.6 a	1.51 a	0.92 a	
3C 442	90 b	20.6 a	6.2 a	3.3 b	1.63 a	0.82 b	
3C 445	118 b	24.8[3] b	8.7 a	5.3 a	3.22 a	2.04 a	
3C 449		11.5 a	5.2 a	3.7 a	2.47 a	1.39 b	
3C 452	200 d	54.4 a	18.5 a	10.3 a	5.87 a	3.26 b	
3C 454	27 d	11.6 a	3.3 b	2.1 a	1.21 a	0.79 a	
3C 454.1		9.8 b	3.0 b	1.6 b	0.65 b	0.22 d	
3C 454.2		8.8 b	3.6 b	2.3 a	1.29 a	0.76 a	
3C 454.3	27 c	13.0 a	12.8*a	10.6*a	11.00*a	18.2 *a	53
3C 455	41 b	12.8 a	4.8 a	2.9 a	1.48 a	0.93 b	
3C 456	32 d	10.6 a	3.9 a	2.5 a	1.33 a	0.67 a	
3C 458	35 c	14.5 a	4.5 a	2.6 a	1.67 a	0.93 b	
3C 459	53 c	25.6 a	7.6 a	4.0 a	2.28 a	1.36 a	
3C 460		10.3[3] c	2.7 b	1.5 b	0.77 b	0.34 b	
3C 461	37200 b	11600. a	3880. a	2410. a	1470. a	910. a	54
3C 465	125 c	37.8[3] a	13.4 a	7.7 a	4.21 a	2.80 a	
3C 468.1		30.0 a	9.7 a	5.0 a	1.93 a	0.87 a	
3C 469.1		12.4[3] b	2.9 b	1.8 b	0.83 b	0.41 b	
3C 470		10.1 a	3.5 b	1.9 b	1.04 a	0.55 b	

NOTES TO TABLE 3

1. 3C 6.1: S_{38} quoted by Williams, Kenderdine, and Baldwin (1966) unreliable due to confusion by 3C 461.

2. 3C 14.1: Consists of two components. Flux densities of 4C 58.02 (NRAO 28) used at all frequencies.

3. 3C 29: Flux densities of 4C −01.05 (NRAO 50, P 0055−01) used at all frequencies. S_{38} uncertain due to confusion by 4C −01.04. (NRAO 49, P 0053−01).

4. 3C 40: Scatter in flux densities probably due to large errors in correction for angular size at the shorter wavelengths.

5. 3C 58: Spectrum unusually flat, but not straight. High polarization at centimeter wavelengths (Sastry, Pauliny-Toth, and Kellermann 1967; Hobbs and Haddock 1967) and low galactic latitude suggest non-thermal source, such as a supernova remnant.

6. 3C 84: Very complex and variable spectrum (Ryle and Windram 1968; Kellermann and Pauliny-Toth 1969).

7. 3C 129: Includes 3C 129.1 at all frequencies.

8. 3C 135: S_{178} seems high; possibly confused by 4C 01.13.

9. 3C 139.1: Thermal spectrum becoming optically thick below 500 MHz. No source detected at all at 38 MHz where the background temperature is 14000° K, so that the electron temperature in 3C 139.1 is estimated to be 14000° ± 1500° K.

10. 3C 144: Tau A. Flux density at 1400 MHz determined from measured ratio to Cas A (Heeschen 1961). Flux density at 5000 MHz determined from measured ratio to Cas A (Baars, Mezger, and Wendker 1965).

11. 3C 147.1: Thermal spectrum becoming optically thick below 1000 MHz. No source detected at all at 38 MHz, but as the background temperature is not accurately known, no electron temperature can be derived. Flux densities at 2695 and 5000 MHz measured by Altenhoff (private communication).

12. 3C 153.1: Thermal spectrum which is optically thin even at 38 MHz.

13. 3C 157: IC 443. Flux densities at 750 and 1400 MHz based on Hogg (1964). Flux density at 2695 interpolated from Hogg's measurements at 1400 and 3000 MHz.

14. 3C 177: Data refer to NRAO 261 (4C 15.19, P 0721+15). 4C 16.21 (P 0721+16) is about 50′ of arc away and forms part of 3C 177.

15. 3C 225: Double source. One component has a low-frequency cutoff near 50 MHz (Macdonald and Kenderdine 1967), resulting in a shoulder in the radio spectrum.

16. 3C 230: Two components, NRAO 339 (4C 00.32, P 0949+00) and NRAO 340 (P 0950+00). Flux density of NRAO 339 alone is 3.0 *a* at 1400 MHz, 1.44 *a* at 2695 MHz, and 0.65 *a* at 5000 MHz.

17. 3C 231: Flat spectrum below 1400 MHz may be due to partial self-absorption. At 2695 MHz at least 10 per cent of the flux comes from a component less than a few seconds in angular diameter (Bash 1968) which may become optically thick at low frequencies.

18. 3C 236: Data are confused by NRAO 346 plus an extended source of emission. See Pauliny-Toth, Wade, and Heeschen (1966) and Fomalont (1968). Flux densities above 750 MHz refer to the small component (Fomalont 1968).

19. 3C 273: Only a lower limit is given to the flux density at 38 MHz, which is confused by 3C 274. The spectrum is complex, consisting of component *A* with a normal spectrum and component *B* containing at least three optically thick components (Kellermann and Pauliny-Toth 1969).

20. 3C 274: Over-all spectrum is remarkably straight, although components with different spectra have been reported (Moffet 1961; Lequeux 1962). Flux densities at 750 and 1400 MHz derived from measured ratios to Cas A (Heeschen 1961).

21. 3C 286: Flat spectrum below 1400 MHz probably due to partial self-absorption.

22. 3C 287: S_{38} includes flux from 4C 25.44, so that there is probably a low-frequency cutoff below 178 MHz in 3C 287.

23. 3C 293: Shoulder between 178 and 750 MHz indicates component with a low-frequency cutoff below 750 MHz. At 2695 MHz 70 per cent of the flux comes from a component less than 3″ in angular diameter (Bash 1968) which may become optically thick at low frequencies.

24. 3C 303.1 and 3C 305.1: These two sources, 15′ of arc apart, have nearly identical flux densities at all frequencies between 178 and 5000 MHz. The two sources are not resolved at 38 MHz, but the combined flux density is considerably less than the flux obtained by extrapolation from the high-frequency spectrum, suggesting a cutoff in both components. This is also suggested by the 81.5-MHz flux densities (Branson 1967). These sources may be similar to 3C 343 and 343.1.

25. 3C 306.1: Data may be confused.

26. 3C 315: Possibly a shoulder between 178 and 750 MHz.

27. 3C 318.1: Steepest spectrum known. Source is not detected at 1400, 2695, and 5000 MHz.

28. 3C 321: Shoulder between 178 and 750 MHz suggests existence of a component with a low-frequency cutoff below 750 MHz.

29. 3C 326: Includes NRAO 485 and NRAO 487 at all frequencies. Flux of NRAO 487 alone is 1.9 *b* at 1400 MHz, 1.3 *b* at 2695 MHz, and 0.48 *a* at 5000 MHz.

30. 3C 326.1: Very marked shoulder between 178 and 750 MHz suggests a major component of small angular size (Fomalont 1968; Bash 1968) with a sharp cutoff near 750 MHz and a high-frequency spec-

tral index near −0.9. In addition, there is a more extended component (Pauliny-Toth, Wade, and Heeschen 1966) which has an index of about −1.3.

31. 3C 327: Possibly a shoulder between 178 and 750 MHz.

32. 3C 343 and 3C 343.1: These two sources are 30′ of arc apart and have nearly identical flux densities at all frequencies, including a sharp cutoff below 178 MHz. Both have extremely small angular diameters and are probably optically thick at low frequencies (Moffet 1965; Williams 1966).

33. 3C 345: Complex spectrum with several optically thick variable components. NRAO 512 is 30′ away, and also has a complex spectrum.

34. 3C 371: Complex variable spectrum with several optically thick components (Kellermann and Pauliny-Toth 1968).

35. 3C 380: Spectral curvature and possible slow variation in flux density at high frequency suggest a component that is optically thick at 5000 MHz.

36. 3C 382: Possibly a shoulder between 178 and 750 MHz.

37. 3C 390.3: Possibly a shoulder between 178 and 750 MHz.

38. 3C 392: W44 (Westerhout 1959). Flux densities at 2695 and 5000 MHz not well determined.

39. 3C 394: Appears to have a low-frequency cutoff below 178 MHz, but region is confused by galactic radiation.

40. 3C 396: Flat non-thermal spectrum in a source at low galactic latitude suggests a supernova remnant.

41. 3C 396.1: Large uncertainties in all flux densities.

42. 3C 397: Non-thermal spectrum. Low-frequency cutoff may be due to absorption by galactic hydrogen. Flux densities at 2695 and 5000 MHz measured by Altenhoff (private communication).

43. 3C 398: The spectrum is flat, although non-thermal. NRAO 598 is only 15′ away and has a thermal spectrum. The source W49 (Westerhout 1959) includes both the thermal (NRAO 598) and non-thermal components (NRAO 599). Flux density at 5000 MHz measured by Altenhoff (private communication).

44. 3C 399.1: Large uncertainties in flux densities due to galactic radiation.

45. 3C 400: Complex H II region. Low apparent flux density at 38 MHz due to high background temperature. No flux density measured at 2695 or 5000 MHz.

46. 3C 403.2: Flux density at 2695 measured by Altenhoff (private communication).

47. 3C 405: Cyg A. Flux densities at 38 and 178 MHz taken from CKL; at 750, 2695, and 1400 MHz, from ratios to Cas A measured by Heeschen (1961); and at 5000 MHz, from ratio to Cas A measured by Baars, Mezger, and Wendker (1965).

48. 3C 418: Spectral curvature suggests component optically thick below 5000 MHz. Some confusion with HB 21.

49. 3C 428: Large uncertainties in flux densities due to galactic radiation.

50. 3C 434.1: Large uncertainties in flux densities due to galactic radiation.

51. 3C 435.1: Includes NRAO 663 and NRAO 664. Flux density of NRAO 663 is 3.6 *b* at 750 MHz, 1.8 *b* at 1400 MHz, 0.97 *a* at 2695 MHz, and 0.7 *b* at 5000 MHz; NRAO 664 is 2.0 *b* at 750 MHz, 1.3 *b* at 1400 MHz, and 0.48 *b* at 2695 MHz.

52. 3C 437.1: Consists of two components, 4C 14.80 (NRAO 668, P 2148+14) and 4C 13.82 (NRAO 669, P 2148+13). Flux densities given are sum of both components. Flux density of 4C 14.80 is 9.6 *b* at 178 MHz, 3.1 *b* at 750 MHz, 2.1 *b* at 1420 MHz, and 1.3 *a* at 2695 MHz.

53. 3C 454.3: Complex spectrum with several optically thick variable components (Kellermann and Pauliny-Toth 1969).

54. 3C 461: Cas A. All flux densities for epoch 1964.4. Flux density at 38 MHz from measurements by Parker (1968). Flux densities at other frequencies obtained from interpolation of absolute measurements given in Table 2.

tainty. The standard error in the spectral index was derived from the deviations of the data from the straight line. This procedure is simple and objective and, for the majority of sources, gives a good fit; moreover, the results are well suited for statistical analysis. However, for sources with marked curvature the results may be misleading. Since a constant index does not describe the spectrum even over these limited ranges of frequencies, the formal errors computed for these sources are large, and as a result the difference between the high- and low-frequency indices may not appear significant in spite of the obvious curvature of the spectrum. For these sources, therefore, we quote values of $\alpha(178\text{–}38)$ or $\alpha(5000\text{–}2695)$ instead of $\alpha(750\text{–}38)$ and $\alpha(5000\text{–}750)$, although the statistical discussion in § V *b* is based entirely on the latter indices. The results are summarized in Table 4 as follows:

Column (1): The source number in the revised 3C catalogue.

Column (2): Optical identification where available. The symbols used are: G for galaxy, QSS for quasi-stellar sources, SNR for supernova remnant, and H II for H II region. Uncertain identifications are noted with a question mark.

Table 4

Spectral Indices

Source	Iden.	α_{38}^{750}		α_{750}^{5000}		Class
3C 2	QSS	-0.67	± 0.01	-0.74	± 0.01	S
3C 6.1		(-0.80	0.08)	-0.89	0.03	C-
3C 9	QSS	-0.99	0.09	-1.02	0.03	S
3C 10	SNR	-0.62	0.03	-0.55	0.02	S
3C 11.1		-0.78	0.17	-0.99	0.04	S
3C 13		-0.93	0.02	-1.08	0.06	S
3C 14	G	-0.77	0.01	-0.91	0.03	C-
3C 14.1		(-0.82	0.08)	-1.06	0.03	C-
3C 15	G	-0.63	0.01	-0.74	0.04	C-
3C 16		-0.85	0.08	-0.94	0.03	S
3C 17	G	-0.63	0.08	-0.66	0.03	S
3C 18	G	-0.68	0.06	-0.71	0.01	S
3C 19		-0.62	0.02	-0.75	0.02	C-
3C 20	G	-0.67	0.01	-0.82	0.02	S
3C 22	G?	-0.75	0.01	-0.89	0.02	C-
3C 27		-0.61	0.03	-0.78	0.04	C-
3C 28	G	-1.01	0.01	-1.22	0.11	S
3C 29	G	-0.77	0.16	-0.65	0.03	?
3C 31	G	-0.59	0.07	-0.68	0.03	S
3C 33	G	-0.67	0.04	-0.74	0.03	S
3C 33.1	G?	-0.69	0.02	-0.94	0.06	C-
3C 33.2		(-0.88	0.10)	-0.86	0.01	S
3C 34		-1.05	0.01	-0.98	0.03	S
3C 35	G	-0.90	0.01	-0.78	0.05	S
3C 36		-0.89	0.04	-1.00	0.04	S
3C 40	G	-0.75	0.06	-0.89	0.03	S
3C 41		-0.55	0.10	-0.68	0.01	S
3C 42		-0.69	0.01	-0.86	0.04	C-
3C 43	QSS	-0.73	0.02	-0.71	0.01	S
3C 44	QSS?	-0.92	0.09	(-1.01	0.01)	S
3C 46	G	-1.01	0.11	-0.95	0.05	S
3C 47	QSS	-0.97	0.02	-0.94	0.02	S
3C 48	QSS	[-0.07	0.07]	-0.80	0.01	C-
3C 49		(-0.62	0.05)	-0.81	0.04	C-
3C 52	G	-0.58	0.05	-0.71	0.03	C-
3C 54		-0.84	0.03	-0.84	0.02	S
3C 55	QSS?	-0.94	0.08	-0.93	0.05	S
3C 58	SNR?	(+0.11	0.03)	-0.10	0.03	?
3C 61.1	G	-0.71	0.02	-0.95	0.03	C-
3C 63	G	-0.83	0.04	-0.92	0.04	S

Table 4 (Continued)

Source	Iden.	α_{38}^{750}	α_{750}^{5000}	Class
3C 65		-0.76 ± 0.04	-1.02 ± 0.04	C-
3C 66	G	-0.70 0.06	-0.72 0.03	S
3C 67	G	(-0.55 0.05)	-0.83 0.05	C-
3C 68.1	G?	-0.80 0.02	-0.86 0.01	S
3C 68.2		-1.11 0.04	-1.35 0.01	C-
3C 69		-0.85 0.03	-1.01 0.05	C-
3C 71	G	-0.53 0.02	-0.71 0.02	C-
3C 75	G	-0.75 0.04	-0.78 0.02	S
3C 76.1	G	-0.70 0.07	-0.62 0.01	S
3C 78	G	-0.51 0.08	-0.54 0.02	S
3C 79	G	-0.77 0.10	-0.98 0.01	C-
3C 83.1	G	-0.72 0.06	-0.68 0.02	S
3C 84	G	-0.93 0.11	[+1.02 0.12]	Cpx
3C 86		-0.65 0.01	-0.60 0.04	S
3C 88	G	-0.58 0.07	-0.69 0.01	S
3C 89	G	-1.00 0.03	-0.98 0.01	S
3C 91		-0.67 0.05	-0.78 0.04	C-
3C 93	QSS	-0.76 0.07	-0.85 0.04	C-
3C 93.1	G	-0.63 0.06	-0.84 0.02	C-
3C 98	G	-0.74 0.01	-0.62 0.03	S
3C 99	G	-0.92 0.20	-0.66 0.06	Cpx
3C 103		-0.78 0.01	-0.95 0.05	C-
3C 105		-0.62 0.05	-0.72 0.04	S
3C 107		-0.90 0.13	-1.02 0.05	C-
3C 109	G	-0.76 0.05	-0.75 0.03	S
3C 111		-0.75 0.02	-0.68 0.02	C+
3C 114	G	-0.90 0.02	-0.92 0.06	S
3C 119	QSS	-0.20 0.03	-0.65 0.03	C-
3C 123	G	-0.69 0.02	-0.79 0.02	C-
3C 124	G	-0.96 0.24	-0.95 0.06	C-
3C 125		-0.90 0.03	-1.02 0.05	S
3C 129	G	-0.89 0.02	-0.94 0.06	C-
3C 130	G	-0.86 0.01	-0.83 0.01	S
3C 131		-0.78 0.01	-0.91 0.04	C-
3C 132	G	-0.67 0.04	-0.86 0.03	C-
3C 133		-0.65 0.01	-0.73 0.02	C-
3C 134		-0.96 0.01	-1.17 0.03	C-
3C 135	G	-0.82 0.07	-0.80 0.07	S
3C 136.1	G	-0.83 0.07	-0.67 0.05	S
3C 137		-0.81 0.12	-0.96 0.09	C-

Table 4 (Continued)

Source	Iden.	α_{38}^{750}		α_{750}^{5000}		Class
3C 138	QSS	[+0.35	± 0.25]	-0.56	± 0.05	C-
3C 139.1	HII	(+0.38	0.10)	(+0.06	0.16)	T
3C 139.2		-0.99	0.02	-0.78	0.08	S
3C 141		-0.85	0.02	-1.05	0.06	C-
3C 142.1		-0.90	0.04	-0.92	0.04	S
3C 144	SNR	-0.30	0.01	-0.26	0.02	S
3C 147	QSS	[+0.77	0.17]	-0.74	0.03	C-
3C 147.1	HII	(+0.84	0.08)	(-0.03	0.05)	T
3C 152		-0.79	0.09	-1.31	0.14	C-
3C 153	G	-0.62	0.02	-0.82	0.05	C-
3C 153.1	HII	+0.24	0.04	(-0.08	0.07)	T
3C 154		-0.77	0.01	-0.71	0.02	S
3C 157	SNR	-0.25	0.10	(-0.25	0.08)	S
3C 158		-0.98	0.07	-0.97	0.02	S
3C 165		-0.73	0.03	-0.98	0.02	C-
3C 166	G	-0.96	0.03	-0.67	0.01	C+
3C 169.1		-0.89	0.01	-0.88	0.11	S
3C 171	G	-0.74	0.08	-0.84	0.03	S
3C 172		-0.75	0.05	-0.89	0.02	C-
3C 173		-0.67	0.08	-0.96	0.05	C-
3C 173.1	G	-0.81	0.04	-0.92	0.03	C-
3C 175	QSS	-0.96	0.02	-1.02	0.01	S
3C 175.1		-0.80	0.12	-0.90	0.07	C-
3C 177	G	-0.90	0.10	-0.89	0.07	S
3C 180	G	-0.81	0.02	-0.81	0.02	S
3C 181	QSS	-0.86	0.09	-0.89	0.04	S
3C 184		-0.74	0.09	-1.00	0.04	C-
3C 184.1	G	-0.66	0.01	-0.76	0.01	C-
3C 186	QSS	-1.02	0.13	-1.08	0.09	S
3C 187		-0.97	0.14	-1.00	0.06	S
3C 190	QSS	-0.80	0.12	-0.86	0.03	S
3C 191	QSS	-0.92	0.04	-1.00	0.05	S
3C 192	G	-0.77	0.04	-0.70	0.02	S
3C 194		-0.75	0.04	-0.89	0.05	C-
3C 196	QSS	-0.68	0.05	-0.88	0.02	C-
3C 196.1	G	-1.09	0.03	-1.05	0.05	S
3C 197.1	G	-0.70	0.01	-0.67	0.05	S
3C 198	G	-0.79	0.10	-1.05	0.05	C-
3C 200	G	-0.85	0.07	-0.89	0.02	S
3C 204	QSS	-1.00	0.04	-1.04	0.09	S

Table 4 (Continued)

Source	Iden.	α_{38}^{750}	α_{750}^{5000}	Class
3C 205	QSS	-0.84 ± 0.01	-0.94 ± 0.06	S
3C 207	QSS	-0.80 0.07	-0.52 0.06	C+
3C 208	QSS	-0.90 0.08	-1.15 0.05	C-
3C 208.1		-0.62 0.05	-0.79 0.03	C-
3C 210	G	-0.80 0.01	-0.96 0.02	C-
3C 212	G	-0.79 0.18	-0.84 0.03	C-
3C 213.1	G	-0.56 0.02	-0.68 0.10	S
3C 215	QSS	-0.94 0.10	-1.00 0.07	S
3C 216	QSS	-0.72 0.06	-0.65 0.06	C+
3C 217	QSS	-0.75 0.02	-1.09 0.06	C-
3C 219	G	-0.74 0.03	-0.93 0.03	C-
3C 220.1	G	-0.82 0.07	-1.10 0.01	C-
3C 220.2		-0.62 0.01	-0.85 0.01	C-
3C 220.3	G	-0.68 0.02	-1.15 0.02	C-
3C 222	G	-1.01 0.23	-1.50 0.15	C-
3C 223	G	-0.71 0.01	-0.73 0.03	S
3C 223.1	G	-0.58 0.04	-0.60 0.01	S
3C 225		-0.80 0.14	-0.95 0.02	C-
3C 226	G	-0.82 0.03	-1.01 0.02	C-
3C 227	G	-0.78 0.03	-0.82 0.02	S
3C 228		-0.80 0.13	-0.83 0.04	S
3C 230		-0.82 0.01	(-0.92 0.03)	S
3C 231	G	-0.25 0.03	-0.54 0.05	C-
3C 234	G	-0.83 0.01	-0.95 0.02	C-
3C 236	G	-0.62 0.05*	-0.70 0.03	S
3C 237	G?	-0.49 0.12	-0.84 0.04	C-
3C 238		-0.76 0.06	-1.11 0.05	C-
3C 239		-0.97 0.07	-1.15 0.02	C-
3C 241		(-0.94 0.08)	-1.14 0.07	C-
3C 244.1	G	-0.80 0.01	-0.94 0.03	C-
3C 245	QSS	-0.72 0.03	-0.67 0.01	S
3C 247		-0.70 0.21	-0.88 0.05	C-
3C 249		-0.81 0.11	-1.04 0.05	C-
3C 249.1	QSS	-0.82 0.03	-0.79 0.04	S
3C 250		-1.00 0.04	-1.16 0.06	C-
3C 252		-1.08 0.06	-1.12 0.05	S
3C 254	QSS	-0.85 0.06	-1.01 0.06	C-
3C 255	G	-0.76 0.12	-1.46 0.08	C-
3C 256		-0.87 0.01	-1.06 0.06	S
3C 257		-0.84 0.01	-0.92 0.03	S

Table 4 (Continued)

Source	Iden.	α_{38}^{750}		α_{750}^{5000}		Class
3C 258	G	(-1.27 ±	0.14)	-0.75 ±	0.11	C+
3C 263	QSS	-0.76	0.02	-0.82	0.01	S
3C 263.1	G	-0.76	0.08	-1.03	0.01	C-
3C 264	G	-0.76	0.04	-0.81	0.02	S
3C 265	G?	-0.91	0.01	-1.10	0.06	C-
3C 266	G	-0.87	0.13	-1.17	0.08	C-
3C 267		-0.81	0.06	-0.94	0.06	C-
3C 268.1		-0.56	0.01	-0.69	0.02	C-
3C 268.2	G	-0.91	0.05	-0.97	0.06	S
3C 268.3		(-0.46	0.05)	-0.85	0.04	C-
3C 268.4	QSS	-0.74	0.01	-0.95	0.07	C-
3C 270	G	-0.53	0.02	-0.57	0.03	S
3C 270.1	QSS	-0.67	0.08	-0.89	0.03	C-
3C 272		-0.83	0.21	-1.02	0.11	S
3C 272.1	G	-0.57	0.01	-0.58	0.02	S
3C 273	QSS	(-0.25	0.05)	[+0.12	0.12]	Cpx
3C 274	G	-0.79	0.01	-0.80	0.01	S
3C 274.1	G	-0.83	0.01	-1.03	0.06	C-
3C 275		-0.61	0.10	-0.92	0.04	C-
3C 275.1	QSS	-0.84	0.13	-0.88	0.02	C-
3C 277		-0.89	0.02	-1.00	0.07	S
3C 277.1	QSS	-0.59	0.08	-0.64	0.03	C-
3C 277.2		-0.96	0.03	-0.92	0.15	S
3C 277.3	G	-0.71	0.03	-0.65	0.04	S
3C 280		-0.72	0.05	-0.86	0.04	C-
3C 280.1	QSS	-0.88	0.16	-1.09	0.11	S
3C 284	G	-0.92	0.01	-0.82	0.03	S
3C 285	G	-0.85	0.04	-0.75	0.06	S
3C 286	QSS	-0.19	0.01	-0.47	0.02	C-
3C 287	QSS	-0.36	0.02	-0.58	0.02	C-
3C 287.1	G	-0.63	0.15	-0.51	0.07	C+
3C 288	G	-0.74	0.07	-0.95	0.03	C-
3C 288.1	QSS	-0.78	0.08	-0.99	0.03	C-
3C 289		-0.71	0.07	-1.00	0.04	C-
3C 293	G	-0.54	0.10	-0.69	0.01	C-
3C 293.1	G	-0.99	0.01	(-1.17	0.02)	S
3C 294		-1.10	0.05	-1.14	0.07	S
3C 295	G	[-0.08	0.06]	-0.90	0.04	C-
3C 296	G	-0.61	0.05	-0.60	0.07	Cpx
3C 297		-0.99	0.02	-0.70	0.03	C+

Table 4 (Continued)

Source	Iden.	α_{38}^{750}		α_{750}^{5000}		Class
3C 298	QSS	[-0.31	± 0.07]	-1.10	± 0.03	C-
3C 299	G	-0.61	0.01	-0.88	0.01	C-
3C 300	G	-0.78	0.04	-0.91	0.02	S
3C 300.1		-0.68	0.01	-0.93	0.10	C-
3C 303		-0.74	0.02	-0.74	0.03	S
3C 303.1		[-0.03	0.20]	-1.07	0.20	C-
3C 305	G	-0.79	0.03	-0.88	0.04	S
3C 305.1		[-0.03	0.20]	-0.92	0.09	C-
3C 306.1	G	-0.82	0.06	-0.88	0.09	S
3C 309.1	QSS	-0.45	0.06	-0.57	0.01	C-
3C 310	G	-0.89	0.01	-1.29	0.06	C-
3C 313	G	-0.84	0.02	-0.81	0.06	S
3C 314.1	G	-0.92	0.01	-1.09	0.10	C-
3C 315	G	-0.79	0.04	-0.86	0.03	S
3C 317	G	-0.92	0.07	-1.36	0.05	C-
3C 318	G	-0.69	0.10	-0.92	0.03	C-
3C 318.1		-1.60	0.13	<-1.9		C-
3C 319	G	-0.81	0.04	-1.02	0.02	S
3C 320	G	-0.74	0.02	-0.96	0.01	C-
3C 321		-0.73	0.09	-0.83	0.01	C-
3C 322	G	-0.73	0.03	-1.08	0.06	C-
3C 323	G?	-0.84	0.01	-1.06	0.01	C-
3C 323.1	QSS	-0.62	0.01	-0.79	0.06	C-
3C 324		-0.82	0.04	-1.05	0.04	C-
3C 325		-0.63	0.04	-1.03	0.09	C-
3C 326	G	-0.73	0.24	(-0.95	0.04)	Cpx
3C 326.1		-0.43	0.29	-1.15	0.10	?
3C 327	G	-0.74	0.12	-0.84	0.03	C-
3C 327.1	G?	-0.81	0.01	-1.01	0.02	C-
3C 330		-0.68	0.01	-0.81	0.03	C-
3C 332	G	-0.63	0.04	-0.83	0.02	C-
3C 334	QSS	-0.97	0.14	-0.97	0.08	S
3C 336	QSS	-0.73	0.04	-0.93	0.05	C-
3C 337		-0.59	0.01	-0.91	0.05	C-
3C 338	G	-1.09	0.05	-1.54	0.02	C-
3C 340		-0.73	0.04	-0.88	0.05	S
3C 341		-0.80	0.01	-1.00	0.06	C-
3C 343		(-0.34	0.05)	-0.84	0.03	C-
3C 343.1		(-0.28	0.05)	-0.99	0.01	C-
3C 345	QSS	-0.30	0.08	[+0.08	0.12]	Cpx

Table 4 (Continued)

Source	Iden.	α_{38}^{750}	α_{750}^{5000}	Class
3C 346	G	-0.53 ± 0.08	-0.65 ± 0.02	Cpx
3C 348	G	-1.00 0.01	-1.03 0.01	S
3C 349	G	-0.76 0.05	-0.77 0.03	S
3C 351	QSS	-0.70 0.01	-0.74 0.02	S
3C 352		-0.84 0.01	-1.05 0.05	C-
3C 353	G	-0.71 0.01	-0.72 0.01	S
3C 356		-0.97 0.02	-0.99 0.07	S
3C 357	G	-0.61 0.05	-0.77 0.06	C-
3C 368		-1.15 0.11	-1.30 0.03	S
3C 371	G	-0.43 0.16	[-0.17 0.12]	Cpx
3C 379.1		-0.76 0.10	-0.74 0.03	S
3C 380	QSS	-0.74 0.04	-0.57 0.04	C+
3C 381	G	-0.68 0.10	-0.76 0.06	C-
3C 382	G	-0.65 0.14	-0.74 0.01	S
3C 386	G	-0.59 0.04	-0.74 0.03	C-
3C 388	G	-0.65 0.01	-0.88 0.01	C-
3C 390		-0.74 0.07	-0.77 0.03	S
3C 390.3	G	-0.70 0.03	-0.78 0.03	S
3C 391		(+0.36 0.08)	-0.57 0.03	C-
3C 392	SNR	-0.36 0.03	(-0.52 0.13)	S
3C 394		(-0.78 0.05)	-0.88 0.06	C-
3C 396		(-0.25 0.10)	(-0.25 0.03)	S
3C 396.1		-0.49 0.18	(-0.46 0.25)	S
3C 397		[+0.28 0.20]	-0.51 0.02	C-
3C 398		(-0.23 0.13)	(-0.34 0.08)	C-
3C 399.1		-0.89 0.10	(-0.78 0.02)	S
3C 399.2		(-0.44 0.08)		
3C 400	HII	(+0.52 0.10)	(-0.16 0.15)	T
3C 400.1		(-0.83 0.08)	-0.74 0.02	S
3C 400.2		-0.64 0.04	(-0.39 0.16)	S
3C 401	G	(-0.68 0.05)	-0.90 0.05	C-
3C 402	G?	(-0.56 0.05)	-0.87 0.10	C-
3C 403	G	-0.52 0.13	-0.80 0.03	S
3C 403.1	G	-1.01 0.08	-0.92 0.09	S
3C 403.2		(+0.20 0.10)	(-0.59 0.16)	C-
3C 405	G	-0.66 0.04	-1.09 0.02	C-
3C 409		-0.78 0.02	-1.11 0.04	C-
3C 410		-0.57 0.03	-0.76 0.02	C-
3C 411		-0.79 0.01	-0.94 0.05	C-
3C 415.2		(-1.02 0.10)	-1.00 0.02	S

Table 4 (Continued)

Source	Iden.	α_{38}^{750}	α_{750}^{5000}	Class
3C 418		(-0.43 ± 0.05)	-0.27 ± 0.06	C+
3C 424	G	-0.85 0.01	-0.98 0.03	S
3C 427.1		-0.92 0.03	-1.07 0.04	C-
3C 428		-0.71 0.09	-1.33 0.15	?
3C 430	G	-0.74 0.04	-0.68 0.03	S
3C 431		-0.94 0.02	-1.15 0.03	C-
3C 432	QSS	-0.95 0.01	-1.07 0.06	C-
3C 433	G	-0.72 0.02	-0.88 0.01	C-
3C 434		-0.63 0.06	-0.85 0.05	C-
3C 434.1		-0.56 0.06	(-0.09 0.14)	?
3C 435		-0.86 0.03	(-0.98 0.07)	S
3C 435.1		-0.53 0.04	(-0.65 0.23)	?
3C 436	G	-0.85 0.06	-0.90 0.02	S
3C 437		-0.74 0.02	-0.92 0.02	C-
3C 437.1		-0.59 0.20	(-0.99 0.15)	C-
3C 438		-0.84 0.03	-1.13 0.02	C-
3C 441	G?	-0.78 0.01	-0.78 0.01	S
3C 442	G	-0.88 0.03	-1.09 0.02	C-
3C 445	G	-0.85 0.08	-0.77 0.01	S
3C 449	G	(-0.55 0.05)	-0.63 0.04	S
3C 452	G	-0.76 0.03	-0.90 0.01	S
3C 454	QSS	-0.81 0.09	-0.76 0.02	S
3C 454.1		(-0.82 0.10)	-1.24 0.10	C-
3C 454.2		(-0.61 0.10)	-0.83 0.01	C-
3C 454.3	QSS	-0.09 0.13	[+0.86 0.13]	Cpx
3C 455	G	-0.70 0.02	-0.90 0.05	C-
3C 456	G	-0.69 0.01	-0.94 0.06	C-
3C 458	G	-0.76 0.07	-0.81 0.03	C-
3C 459	G	-0.74 0.11	-0.91 0.03	C-
3C 460	G	(-0.93 0.14)	-1.07 0.06	S
3C 461	SNR	-0.76 0.01	-0.77 0.01	S
3C 465	G	-0.72 0.02	-0.84 0.04	C-
3C 468.1		(-0.78 0.05)	-1.29 0.06	C-
3C 469.1		(-1.01 0.10)	-1.04 0.07	S
3C 470	G	(-0.72 0.08)	-0.97 0.02	C-

* No 38 or 750 MHz flux density. Index quoted is between 178 MHz and 1400 MHz.

Column (3): The spectral index, $\alpha(750\text{–}38)$, determined between 38 and 750 MHz; if the spectrum shows a sharp cut-off at frequencies below 178 MHz (e.g., 3C 48, 3C 138, and 3C 147), the value of $\alpha(138\text{–}38)$ is given in square brackets. If the flux density at 38 MHz is unavailable, the low-frequency spectral index has been determined between 178 and 750 MHz only, and this is indicated by quoting the index in round brackets.

Column (4): The spectral index, $\alpha(5000\text{–}750)$, determined between 750 and 5000 MHz; if the spectrum shows a large departure from a power law (e.g., 3C 84, 3C 273, and 3C 454.3), the value of $\alpha(5000\text{–}2695)$ is given in square brackets. Where one or two of the flux densities in this range are not available, the index is given in round brackets.

Column (5): A qualitative classification describing the form of the spectrum as defined in the next section. In classifying the spectra we have occasionally used flux densities at 10 MHz (Bridle and Purton 1968) and at 405 MHz and 15 GHz (Kellermann and Pauliny-Toth unpublished). Accurate flux densities were also available at 81.5 MHz for sources at declinations greater than +70° (Branson 1967).

a) Classification of Radio Spectra

The various classes of radio spectra are illustrated in Figures 2, 3, 4, and 5, and are discussed below.

i) *Class S*

For some sources, the spectrum over the whole frequency range can be described by a simple power law, so that if log (S_ν) is plotted against log (ν), the data lie on a straight line (see Figs. 1 and 2); the spectrum of such a source is therefore described as "straight." With the increased accuracy of flux-density measurements over a frequency range of 125:1, the proportion of sources which do not show a significant departure from a simple power law is smaller than the CKL study had suggested. It is remarkable, however, that for about 40 per cent of sources the radiation should follow a simple power law so accurately over such a large frequency range. This implies a well-defined power-law distribution in electron energy which must be accounted for in any proposed mechanism for the production of relativistic particles. It is especially surprising that some sources, such as Vir A (3C 274), have an over-all spectrum which follows a simple power law, although they are known to contain several components with apparently different spectra (Moffet 1961; Lequeux 1962).

As sources with straight spectra are especially useful for calibration purposes, a selection of these sources is listed in Table 5, giving the best-fitting spectral index between 38 and 5000 MHz and the flux density at 1000 MHz.

ii) *Class C– (Convex Spectra)*

In a large proportion of sources $|\alpha(750\text{–}38)|$ is significantly smaller than $|\alpha(5000\text{–}750)|$, and the spectra of such sources are described as having negative curvature (see Fig. 3). In most cases this does not appear to be the result of a gradual curvature over the whole frequency range; instead, there appears to be a well-defined power-law spectrum above the frequency of maximum curvature, and often the data below this frequency are compatible with another flatter power-law spectrum, although the larger errors at low frequencies may disguise any further curvature. The frequency of maximum curvature often appears to lie between 750 and 1400 MHz, though this may partly depend on the selection of frequencies used in the present study.

In a few cases there is a very sharp cutoff in the spectrum at low frequencies (e.g., 3C 48, 3C 147, and 3C 298, Fig. 4). Such spectra are always associated with sources of extremely high brightness temperature, and it is probable that the cutoff is due to synchrotron self-absorption (Slish 1963; Williams 1963).

iii) *Class C+ (Concave Spectra)*

In a few sources, $|\alpha(750\text{–}38)|$ is significantly larger than $|\alpha(5000\text{–}750)|$, and the spectra of such sources are described as having positive curvature (see Fig. 5). In some

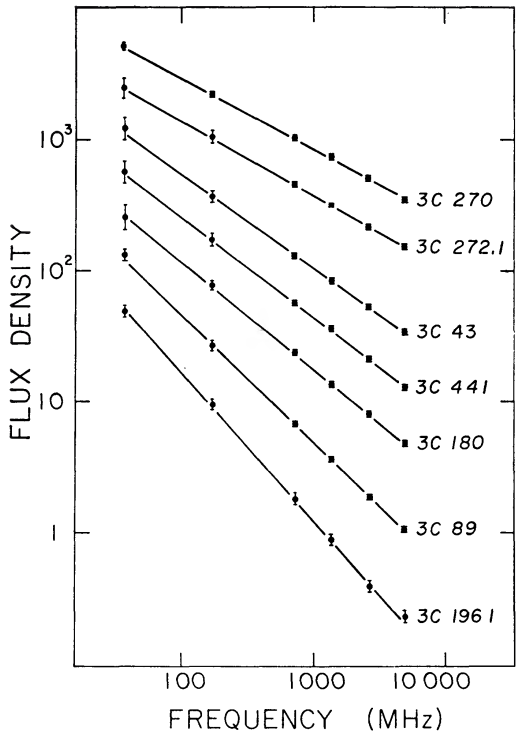

FIG. 2

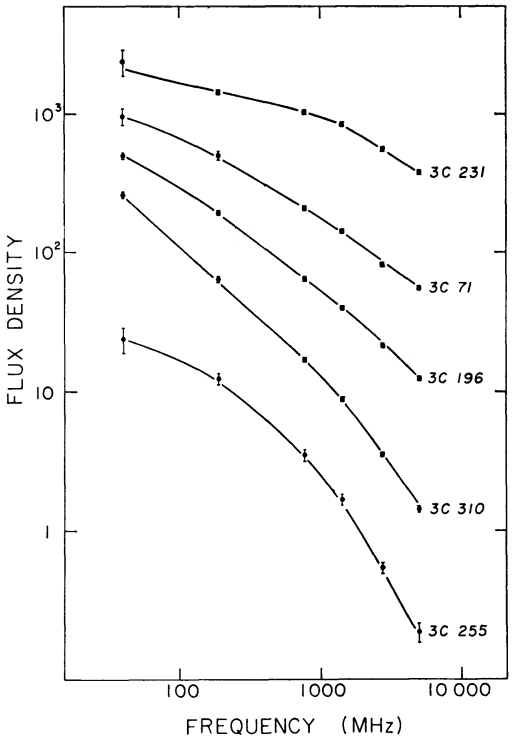

FIG. 3

FIG. 2.—Spectra of some sources with constant spectral indices. Vertical scale is arbitrary.
FIG. 3.—Spectra of some sources with negative curvature. Vertical scale is arbitrary.

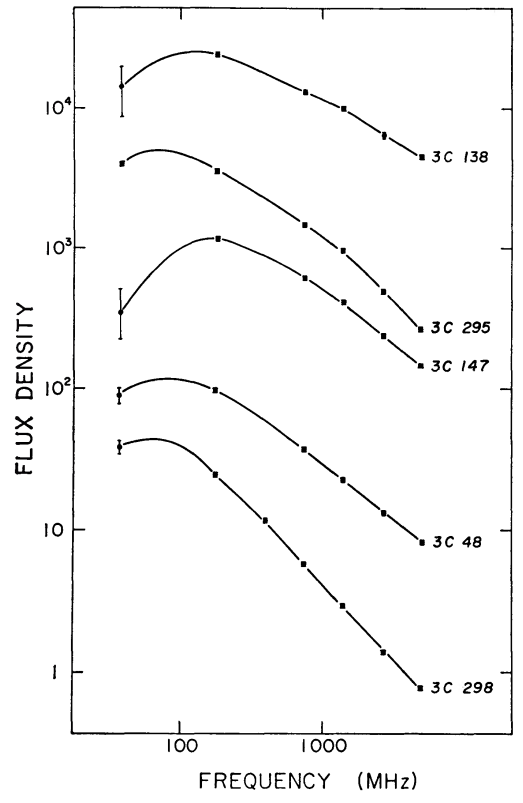

FIG 4

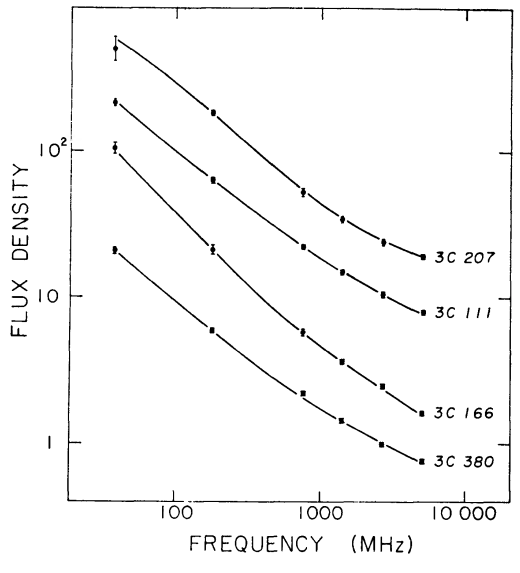

FIG. 5

FIG. 4.—Spectra of some sources which show a sharp low-frequency cutoff. Vertical scale is arbitrary.
FIG. 5.—Spectra of some sources which have positive curvature. Vertical scale is arbitrary.

cases the source is known to consist of two components, one with a flat spectrum which dominates at high frequencies and the other with a steep spectrum which dominates at low frequencies. Whenever the different components of a complex source have significantly different spectral indices, the over-all spectrum will show positive curvature. In fact, very few 3C sources behave in this way, and this suggests that when a source is made up of several components, the spectral indices and thus the electron-energy distributions of the various components are usually similar.

iv) *Class Cpx*

Several sources show more complex spectra and we have classified these as Complex. Most of these are thought to be composite spectra caused by two or more components

TABLE 5

SPECTRA OF RADIO SOURCES SUITABLE FOR CALIBRATION

a) Primary standard (based on absolute measurements):		
3C 461 (Cas A)	$\alpha = -0.765 \pm 0\ 005$	$S_{1000} = 3090 \pm 30$ f.u.
b) Secondary standards (based on direct comparison with Cas A):		
3C 218	$\alpha = -0\ 91 \pm 0\ 01$	$S_{1000} = 58\ 0$ f.u.
274	$-0\ 80 \pm 0\ 01$	266.
348	$-1.02 \pm 0\ 01$	60 0
353	$-0\ 71 \pm 0.01$	70 0
c) Provisional standards (based on direct comparison with *b*):		
3C 43	$\alpha = -0\ 71 \pm 0\ 01$	$S_{1000} = 3.48$ f.u.
47	$-0\ 96 \pm 0\ 01$	5 13
75	$-0\ 73 \pm 0\ 01$	7 73
89	$-0\ 99 \pm 0.01$	3 81
130	$-0\ 82 \pm 0\ 01$	3 40
175	-0.98 ± 0.01	3.31
180	$-0.82 \pm 0\ 01$	3 46
196 1	$-1\ 09 \pm 0\ 01$	2 63
197 1	$-0\ 69 \pm 0\ 02$	2 44
223	$-0\ 73 \pm 0\ 01$	4 10
223 1	$-0\ 59 \pm 0\ 01$	2.23
227	$-0.79 \pm 0\ 01$	9 10
249.1	$-0\ 80 \pm 0\ 02$	2 94
263	$-0\ 79 \pm 0\ 01$	3.88
270	-0.54 ± 0.01	21.0
272.1	$-0.58 \pm 0\ 01$	7.10
303	-0.74 ± 0.01	3 18
349	-0.75 ± 0.02	3 86
351	$-0\ 71 \pm 0\ 01$	4 13
441	$-0\ 78 \pm 0.01$	3 26

with different spectra. For example, some sources have a "shoulder" in the spectrum (that is, the indices at low and high frequencies are nearly equal, but the flux densities at lower frequencies are systematically lower than the values predicted by extrapolating the spectrum at high frequencies); this is often confirmed by the flux densities measured at 10 and 405 MHz. It is suggested that in such sources there are two components with about equal intensities and equal spectral indices at high frequencies, but in one component there is a low frequency cutoff within the frequency range of the present analysis, so that at frequencies below the cutoff frequency only the other component is observed. In at least two such sources, 3C 225 and 3C 267, this interpretation is supported by observations made with the Cambridge 1-mile telescope which shows in each case a component of small angular diameter with a low-frequency cutoff below about 200 MHz (Macdonald and Kenderdine 1967). More complete spectral data at the lower frequencies, particularly below 38 MHz, would probably disclose further examples of this type, which with the present data are classified as C−.

For a few sources the spectra are extremely complex with several maxima and minima.

Such spectra are probably the sum of a number of components each of which has a cutoff at a different frequency. Sources 3C 84, 3C 273, 3C 345, and 3C 454.3 have spectra of this type. These and other similar sources, which often show large time variations, are discussed elsewhere in more detail (Kellermann and Pauliny-Toth 1969).

v) *Class T*

Sources classified as having thermal spectra are found close to the galactic plane, and without doubt these are galactic H II regions. In most cases the sources are optically thick at the longer wavelengths, though in a few cases the emission measure is small and the flux density of the source remains constant down to 38 MHz. In interpreting the apparent spectrum of a thermal source, it must be remembered that at wavelengths where the source is optically thick, the background radiation observed through the source is attenuated by absorption so that the apparent flux density of an optically thick source, measured with respect to the surrounding background radiation, will be less than the true flux density.

b) Spectral Curvature

It is clear from Table 4 that for the majority of sources at high galactic latitudes the spectra are steeper at high frequencies, with a mean difference of about 0.12 between the indices. Such a curvature may partly be due to systematic errors in the calibration of the flux-density scales in the different frequency ranges, but this is unlikely to account for the observed degree of curvature. For example, it would be possible to explain a difference of 0.12 between the indices if the flux densities at 38 and 178 MHz were systematically low by 40 and 18 per cent, respectively, or if the flux densities at 1400, 2695, and 5000 MHz were low by 8, 18 and 25 per cent, respectively: Such errors are far larger than the estimated uncertainties in the calibration.

The probable cause of this curvature in the spectrum is suggested when the brightness temperature of each source is considered. It has been known for some time that certain sources of very small angular diameter and hence of high surface brightness have highly curved spectra (Kellermann *et al.* 1962). In some sources of small angular size, the cutoff at low frequencies is very sharp; these include the quasi-stellar sources 3C 48, 3C 119, 3C 138, 3C 147, and 3C 298; the radio galaxy 3C 295; and the unidentified sources 3C 49, 3C 303.1, 3C 305.1, and 3C 343 and 343.1. Apparently these are relatively simple sources in which most of the emission originates in a component of uniformly high surface brightness so that absorption by the relativistic electrons causes the source to become optically thick below a well-defined cutoff frequency. In such sources the frequency at which the flux density is a maximum, ν_m(MHz), is determined by the angular diameter of the source, θ, and the magnetic field within the source, B (in gauss), as given by the relation,

$$\theta^2 = f(\gamma)B^{1/2}S(\nu)\nu^{(\gamma-1)/2}\nu_m^{-(4+\gamma)/2}(1+z)^{1/2}(\text{sec of arc})^2 ,$$

where S is the flux density in flux units at a frequency ν where the optical depth is small, $\gamma = 1\text{–}2\alpha$, $f(\gamma) = 6.4 \times 10^3$ for $\gamma = 1.5$ and 4.5×10^3 for $\gamma = 2.5$, and z is the redshift of the source.

Another straightforward example occurs when a source consists of two components with populations of relativistic electrons having similar energy spectra, but with very different brightness temperatures. In such a source, the component with the higher brightness temperature will cut off at a higher frequency, so that, as described in § V, the low-frequency spectrum has the same slope as the high-frequency spectrum but corresponds to one component only.

Some sources are even more complex. Several with a sharp cutoff, such as 3C 48 and 3C 295, sometimes show a definite flattening of the spectrum at frequencies as much as 10 times higher than the cutoff frequency. In other sources there is a gradual flatten-

ing of the slope but no sharp cutoff, at least above 38 MHz. In order that self-absorption should produce a flattening of the spectrum over such a wide range of frequencies, different parts of the source must become optically thick at different frequencies, a condition which implies an extremely wide range of brightness temperature. Interferometer observations do provide direct evidence that some sources of relatively low average brightness temperature contain very small, bright components (Wade 1966; Bash 1968). There are, however, insufficient high-resolution interferometric data to allow a detailed comparison of spectral curvature and surface brightness. Nevertheless, some estimate of the extent of small-scale structure in extended sources is provided by observations of interplanetary scintillations which are detected when sources containing structure of the order of 1″ or less pass behind the solar corona (e.g., Williams 1964; Hewish, Scott, and Wills 1964).

Of eighty-seven sources selected at random from the revised 3C catalogue and which pass close to the sun, forty-two have a scintillating component of 20 per cent or more at 178 MHz, a fact which indicates that at least 20 per cent of the emission is confined to a diameter of 1″ or less (Little and Hewish 1968). The mean spectral index at high frequencies $\alpha(5000\text{–}750) = -0.88 \pm 0.04$ for these scintillating sources, while at low frequencies the mean index $\alpha(750\text{–}38) = -0.66 \pm 0.04$. For the sources which do not contain a scintillating component, the respective indices are -0.83 ± 0.03 and -0.78 ± 0.02, so that the observed spectral curvature appears to be largely confined to sources which contain components of very small diameter and high surface brightness. Some of the curvature found in the non-scintillating sources may also be caused by self-absorption in components where the optical depth is so great that the flux density at 178 MHz is too low for the scintillations to be detected.

We therefore conclude that the form of the radio spectrum in many sources is determined not only by the energy distribution of the relativistic electrons but partly by synchrotron self-absorption in components with a large range of brightness temperatures. The observed range of indices is determined by both factors, and consequently sets an upper limit to the range of indices of the differential energy spectrum of the electrons. It might be expected, therefore, that in the frequency range 750–5000 MHz, where synchrotron self-absorption is less likely to be a factor, the observed range of spectral indices would be smaller. In fact it is larger, suggesting that at high frequencies the original energy distribution of relativistic electrons might be modified by some other mechanism, such as synchrotron radiation losses or inverse Compton scattering. These mechanisms cause a steepening of the spectrum at high frequencies, and therefore may make a contribution to the observed spectral curvature.

c) Comparison of Radio Galaxies and Quasi-stellar Sources

In Figure 6 we have plotted histograms of the distribution of $\alpha(750\text{–}38)$, and $\alpha(5000\text{–}750)$ separately for radio galaxies, quasi-stellar sources, and unidentified sources away from the galactic plane ($b^{II} > 10°$). The mean value of the index, $\langle\alpha\rangle$, and its dispersion, $\Delta\alpha$, are shown in Table 6 for each group. Sources with uncertain identifications are not included in Figure 6 or Table 6. Each of the curves in Figure 6 has been broadened by about 10 per cent by the uncertainties in the individual spectral indices.

In both frequency ranges the mean index for quasi-stellar sources is more positive than for radio galaxies (Williams and Collins 1967) and the dispersion is greater. This difference is entirely due to a small proportion of quasi-stellar sources which have unusually flat spectra; these have angular diameters well under 1″, and in these sources at least we can be certain that synchrotron self-absorption has made a major contribution to the flattening of the spectrum at low frequencies. Apart from these few sources it is clear that for the great majority of quasi-stellar sources in the revised 3C catalogue the distribution of spectral indices is very similar to the distribution for radio galaxies. This is discussed further by Kellermann, Pauliny-Toth, and Tyler (1968) and by Pauliny-Toth and Kellermann (1968). The second population of quasi-stellar sources,

those with very flat spectra, are found in greater numbers in surveys made at higher frequencies, such as the 408-MHz Parkes surveys.

The unidentified sources in the revised 3C catalogue are found to have systematically steeper spectra than either the radio galaxies or the quasi-stellar sources, especially above 750 MHz. As has been pointed out elsewhere (Pauliny-Toth and Kellermann 1968), it is unlikely that the steeper spectra found for the unidentified sources are due

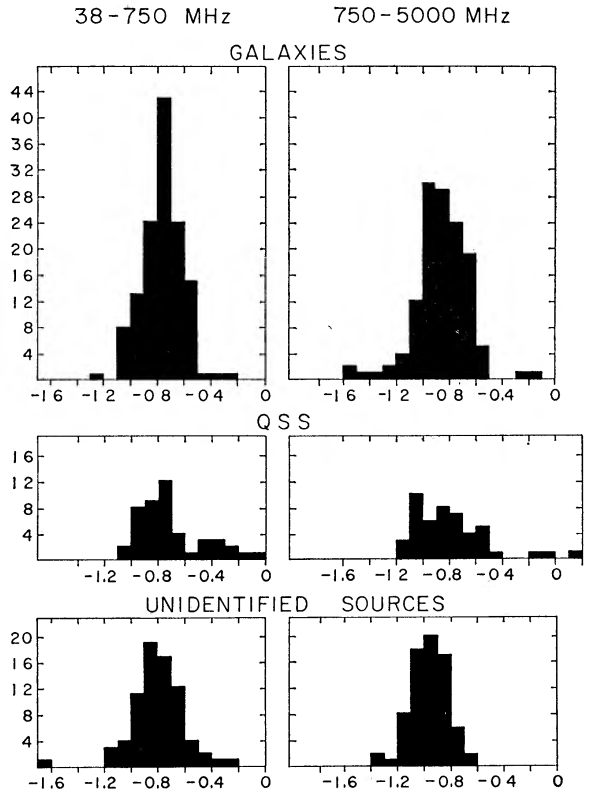

FIG. 6.—Histograms showing the distribution of spectral indices for (*a*) radio galaxies between 38 and 750 MHz, (*b*) radio galaxies between 750 and 5000 MHz, (*c*) quasi-stellar sources between 38 and 750 MHz, (*d*) quasi-stellar sources between 750 and 5000 MHz, (*e*) the unidentified sources with $|b^{II}| \geq 10°$ between 38 and 750 MHz, and (*f*) the unidentified sources between 750 and 5000 MHz.

TABLE 6

MEAN SPECTRAL INDEX AND DISPERSION FOR THE THREE GROUPS OF SOURCES

	38–750 MHz	750–5000 MHz
Galaxies	$\langle\alpha\rangle = -0.753 \pm 0.013$ $\Delta\alpha = 0.149 \pm 0.009$	$\langle\alpha\rangle = -0.851 \pm 0.018$ $\Delta\alpha = 0.204 \pm 0.012$
QSSs	$\langle\alpha\rangle = -0.700 \pm 0.035$ $\Delta\alpha = 0.242 \pm 0.033$	$\langle\alpha\rangle = -0.789 \pm 0.042$ $\Delta\alpha = 0.289 \pm 0.039$
Unidentified Sources	$\langle\alpha\rangle = -0.795 \pm 0.022$ $\Delta\alpha = 0.193 \pm 0.014$	$\langle\alpha\rangle = -0.969 \pm 0.020$ $\Delta\alpha = 0.177 \pm 0.013$

to the large redshift of distant galaxies or quasi-stellar sources causing a shift of the spectrum to lower frequencies. More likely this effect is due to the correlation discussed below between intrinsic luminosity and spectral indices.

d) Spectral Index–Luminosity Relation

In previous spectral studies there has been the suggestion that the spectral index is correlated with luminosity (e.g., Heeschen 1960; CKL). Now that redshifts are available for a greater number of sources and the spectra are known more accurately, we have again compared the spectral index with luminosity, using the absolute power at 178 MHz and α(5000–750). The high-frequency index was chosen for comparison since the effect of self-absorption is relatively small, and the value of α(5000–750) should be representative of the slope, γ, of the electron-energy distribution. Since the list of identifications and redshifts for sources in the revised 3C catalogue is essentially complete to a given photographic magnitude, it is not believed that any selection effect could introduce a false correlation between these two parameters. The new data confirm the fact that, although the dispersion is large, the intrinsically weaker radio galaxies have, on the average, flatter spectra than the stronger ones (see Table 7). The strong radio galaxies then

TABLE 7

RELATION BETWEEN RADIO LUMINOSITY AND SPECTRAL INDEX

Radiated Power at 178 MHz (W Hz^{-1})	Mean Spectral Index
$<10^{24}$	-0.52 ± 0.03
10^{24}–10^{25}	-0.77 ± 0.06
10^{25}–10^{26}	-0.77 ± 0.06
10^{26}–10^{27}	-0.89 ± 0.05
10^{27}–10^{28}	-0.90 ± 0.04
10^{28}–10^{29}	-0.98 ± 0.08

appear to have a deficiency of high-energy electrons compared with the weaker ones. Finally, the spectra of the quasi-stellar sources show no such dependence, although the range of observed luminosities in this case is far smaller.

The tendency for intrinsically strong radio galaxies to have steeper spectral indices probably accounts for the steep spectra found for unidentified sources, since in any sample taken from a relatively narrow range of flux densities, the most luminous sources will be the most distant and thus least likely to be optically identified.

e) Galactic Sources

At various times it has been suggested that a large proportion of observed radio sources might be associated with our own Galaxy. We have obtained the spectral-index distributions for sources observed at different galactic latitudes and find that apart from areas of sky within a few degrees of the galactic plane where the presence of supernova remnants and HII regions alters the distribution, there is no evidence of any dependence of the observed spectrum of radio sources on galactic latitude. The known or suspected remnants of supernovae show a wide range of spectral indices, and in no case is there a significant departure from a power-law spectrum. Self-absorption, therefore, does not affect the radio spectra of the galactic supernovae remnants, and the spectral index of these sources is determined solely by the index of the electron-energy distribution, which must lie in the range $1 < \gamma < 3$ with roughly equal probability.

The large dispersion and essentially constant spectral indices found for the supernova remnants may be contrasted with the spectrum of the galactic background which

is nearly uniform over the sky and which does not follow a simple-power-law distribution (e.g., Andrew 1966; Purton 1966; Bridle 1967).

We would like to thank Drs. Altenhoff, Caswell, and Collins, who generously contributed data in advance of publication. Two of us (K. I. K. and I. P. T.) would like to thank Professor M. Ryle for his hospitality during their stay at the Cavendish Laboratory. Part of this work was done while one of us (K. I. K.) was at the Leiden Observatory with the support of a grant from the Netherlands Organization for the Advancement of Pure Research.

REFERENCES

Allen, R. J., and Barrett, A. H. 1967. *Ap. J.*, **149**, 1.
Andrew, B. H. 1966, *M.N.R.A.S.*, **132**, 79.
Baars, J. W. M., Mezger, P. G., and Wendker, H. 1965, *Ap. J.*, **142**, 122.
Bash, F. N. 1968, *Ap. J.*, **152**, 375.
Bennett, A. S. 1962, *Mem. R.A.S.*, **68**, 163.
Bologna, J. M., McClain, E. F., Rose, W. K., and Sloanaker, R. M. 1965, *Ap. J.*, **142**, 106.
Bolton, J. G., Gardner, F. F., and Mackey, M. B. 1964, *Australian J. Phys.*, **17**, 340.
Branson, N. J. B. A. 1967, *M.N.R.A.S.*, **135**, 149.
Bridle, A. H. 1967, *M.N.R.A.S.*, **136**, 219.
Bridle, A. H., and Purton, C. R. 1968, *A.J.*, **73**, 717.
Clarke, M. E. 1965, *Observatory*, **85**, 67.
Conway, R. G., Kellermann, K. I., and Long, R. J. 1963, *M.N.R.A.S.*, **125**, 261.
Crowther, J. H., and Clarke, R. W. 1966, *M.N.R.A.S.*, **132**, 405.
Day, G. A., Shimmins, A. J., Ekers, R. D., and Cole, D. J. 1966, *Australian J. Phys.*, **19**, 35.
Dent, W. A., and Haddock, F. T. 1966, *Ap. J.*, **144**, 568.
Findlay, J. W., Hvatum, H., and Waltman, W. B. 1965, *Ap. J.*, **141**, 873.
Fomalont, E. B. 1968, *Ap. J. Suppl.*, **15**, 203.
Gower, J. F. R., Scott, P. F., and Wills, D. 1967, *Mem. R. A. S.*, **71**, 49.
Heeschen, D. S. 1960, *Pub. A.S.P.*, **72**, 368.
———. 1961, *Ap. J.*, **133**, 322.
Heeschen, D. S., and Meredith, B. L. 1961, *Pub. N.R.A.O.*, Vol. **1**, No. 8.
Hewish, A., Scott, P. F., and Wills, D. 1964, *Nature*, **203**, 1214.
Hobbs, R. W., and Haddock, F. T. 1967, *Ap. J.*, **147**, 908.
Hogg, D. E. 1964, *Ap. J.*, **140**, 992.
Howard, W. E., Dennis, T. R., Maran, S. P., and Aller, H. D. 1965, *Ap. J. Suppl.*, **10**, 331.
Kellermann, K. I. 1964, *A.J.*, **69**, 205.
Kellermann, K. I., Long, R. J., Allen, L. R., and Moran, M. 1962, *Nature*, **195**, 692.
Kellermann, K. I., and Pauliny-Toth, I. I. K. 1969, *Ap. J. (Letters)*, **155**, L71.
Kellermann, K. I., Pauliny-Toth, I. I. K., and Tyler, W. C. 1968, *A.J.*, **73**, 298.
Khrulev, V. V. 1963, *Radiophysica*, **6**, 398.
Lastochkin, V. P., Porfiriev, V. A., Stankevich, K. S., Troitsky, V. S., Kholodilov, N. N., and Tseitlin, N. M. 1963, *Radiophysica*, **6**, 629.
Lequeux, J. 1962, *Ann. d'ap.*, **25**, 221.
Little, L. T., and Hewish, A 1968, *M.N.R.A.S.*, **138**, 393.
Long, R. J., Smith, M. A., Stewart, P., and Williams, P. J. S. 1966, *M.N.R.A.S.*, **134**, 371.
Macdonald, G. H., and Kenderdine, S. 1967, *Nature*, **215**, 603.
MacRae, D. A., and Seaquist, E. R. 1963, *A.J.*, **68**, 77.
Medd, W. J., and Ramana, K. V. V. 1965, *Ap. J.*, **142**, 383.
Mezger, P. G., and Schraml, J. 1966, *A.J.*, **71**, 864.
Moffet, A. T. 1961, *A.J.*, **66**, 49.
———. 1965, *Ap. J.*, **141**, 1580.
Parker, E. A. 1968, *M.N.R.A.S.*, **138**, 407.
Pauliny-Toth, I. I. K., and Kellermann, K. I. 1968, *A.J.*, **73**, 953.
Pauliny-Toth, I. I. K., Wade, C. M., and Heeschen, D. S. 1966, *Ap. J. Suppl.*, **13**, 65.
Penzias, A. A., and Wilson, R. W. 1965, *Ap. J*, **142**, 1149.
Pilkington, J. D. H., and Scott, P. F. 1965, *Mem. R.A.S.*, **69**, 183.
Price, R. M., and Milne, D. K. 1965, *Australian J. Phys.*, **18**, 329.
Purton, C. R. 1966, *M.N.R.A.S.*, **133**, 463.
Ryle, M., and Windram, M. D. 1968, *M.N.R.A.S.*, **138**, 1.
Sastry, Ch. V., Pauliny-Toth, I. I. K., and Kellermann, K. I. 1967, *A.J.*, **72**, 230.
Shimmins, A. J., Day, G. A., Ekers, R. D., and Cole, D. J. 1966, *Australian J. Phys.*, **19**, 837.
Slish, V. I. 1963, *Nature*, **199**, 682.

Stankevich, K. S. 1963, *Soviet Astr.—AJ*, **6**, 480.
Wade, C. M. 1966, *Phys. Rev. Letters*, **17**, 1061.
Westerhout, G. 1959, *B.A.N.*, **14**, 215.
Williams, P. J. S. 1963, *Nature*, **200**, 56.
———. 1964, unpublished Ph.D. Thesis, Cambridge University.
———. 1966, *Observatory*, **86**, 67.
Williams, P. J. S., and Collins, R. A. 1967, *Observatory*, **87**, 108.
Williams, P. J. S., Collins, R. A., Caswell, J. L., and Holden, D. J. 1968, *M.N.R.A.S.*, **139**, 289.
Williams, P. J. S., Kenderdine, S., and Baldwin, J. E. 1966, *Mem. R.A.S.*, **70**, 53.
Williams, P. J. S., and Stewart, P. 1967, *M.N.R.A.S.*, **135**, 319.
Wills, D., and Parker, E. A. 1966, *M.N.R.A.S.*, **131**, 503.
Wilson, R. W., and Penzias, A. A. 1966, *Ap. J.*, **146**, 286.
Wyllie, D. V. 1969, *M.N.R.A.S.*, **142**, 229.